15,000 Years of mass-movement history in Lake Lucerne: Implications for seismic and tsunami hazards

MICHAEL SCHNELLMANN[1*], FLAVIO S. ANSELMETTI[1], DOMENICO GIARDINI[2] & JUDITH A. MCKENZIE[1]

Key words: Mass-flow deposits, megaturbidites, lacustrine sedimentation, natural hazard, paleoseismology, seismic stratigraphy, Central Switzerland

ABSTRACT

A chronological catalogue of Late Glacial and Holocene mass-movement deposits in Chrüztrichter and Vitznau Basins of Lake Lucerne (Vierwaldstättersee) reveals a complex history of natural hazards affecting the lake and its shores. Ninety-one mass-flow and six megaturbidite deposits have been identified and mapped out with a grid of more than 300 km high-resolution seismic profiles. An age model based on the analyses of 10 long piston cores, 2 tephra layers and 32 AMS-^{14}C ages allowed building up a chronological event catalogue covering the last 15,000 years. Most of the identified mass-flow deposits relate to subaqueous sliding and subaerial rockfalling, as indicated by slide scars and rockfall cones on the lake floor. Deposits related to subaqueous sliding occur at the toe of slopes with inclinations >10° and reach their largest extents below slopes with inclinations between 10 and 20°. On subaqueous slopes >25° there is hardly any sediment accumulation. Rockfall cones and related mass-flow deposits in the northeastern and southern part of Vitznau basin evidence repeated rockfall activity, particularly along two zones on the northern face of Bürgenstock Mountain. Historic examples indicate that such rockfalls, as well as large subaqueous slides, can induce considerable tsunami waves in the lake. All of the 91 identified mass-flow deposits are associated with 19 seismic-stratigraphic event horizons. One of them comprises 13 mass-flow deposits and 2 megaturbidites and relates to the 1601 A.D. $M_w \sim 6.2$ earthquake. By analogy, five older multiple mass-movement horizons, each including six or more coeval deposits, are interpreted to result from strong prehistoric earthquakes.

ZUSAMMENFASSUNG

Ein chronologischer Katalog von Rutschungsablagerungen im Untergrund von 2 Becken des Vierwaldstättersees (Chrüztrichter und Vitznaubecken) zeugt von verschiedenen Naturgefahren, welche den See und dessen Ufer beeinträchtigen. Mit Hilfe eines dichten Netzes von mehr als 300 km hochauflösender reflektions-seismischer Profile wurden subaquatische Abrisskanten, Bergsturzfächer, sowie 91 Rutschungs- und 6 grosse Turbiditablagerungen identifiziert und mit seismisch-stratigraphischen Methoden auskartiert. Die Analyse von 10 Langkernen, zwei Aschenlagen und 32 AMS-[14]C Datierungen ermöglichten eine Altersbestimmung der Ereignisse und das Erstellen eines chronologischen Ereignis-Kataloges der letzten 15,000 Jahre. Die häufigsten und umfangreichsten subaquatischen Rutschungsablagerungen treten am Fuss von Hängen mit einer Neigung von 10-20° auf. Flachere Hänge sind meist stabil und Hänge >25° in der Regel zu steil, um genügend Material für grosse Rutschungen zu akkumulieren. Bergsturzfächer und vorgelagerte Rutschungsablagerungen im Vitznauerbecken deuten auf wiederholte Bergsturzaktivität hin, insbesondere entlang zweier Zonen am Nordabhang des Bürgenstocks. Historische Beispiele zeigen, dass solche Bergstürze sowie grosse subaquatische Rutschungen im See beträchtliche Flutwellen auslösen können. Die identifizierten 91 Rutschungsablagerungen und 6 Turbidite verteilen sich auf 19 seismisch-stratigraphische Ereignis-Horizonte. Ein Ereignis-Horizont, welcher 13 Rutschungsablagerungen und zwei Megaturbidite umfasst, wurde in Zusammenhang mit dem historisch gut dokumentierten Erdbeben im Jahr 1601 abgelagert. Analog werden fünf prähistorische multiple Rutschungsablagerungen ebenfalls starken Erdbeben zugeschrieben.

1. Introduction

Recurrance times are crucial parameters for the assessment of natural hazards, such as earthquakes, rockfalls or floods. The available time series analyses are closely bound to the existence of written historical documents, which, in most of Central and Northern Europe, are limited to the last 400 to maximal 1000 years. This time span is too short to provide sufficient knowledge about the temporal and spatial distribution of rare high-impact events, such as strong earthquakes or major rockfalls. In order to achieve a more complete hazard assessment including such low-frequency events, the historic event catalogue needs to be extended to prehistoric times.

Lakes provide ideal sedimentary archives, which, in contrast to most subaerial archives, are spatially and temporally continuous and can readily be dated. Characteristic event beds in lacustrine sediments have been allocated to historically described catastrophic events, such as floods (e.g. Siegenthaler & Sturm 1991a; Gilli et al. 2003; Bussmann 2006), subaerial debris

* Correspondence: E-mail: michael.schnellmann@alumni.ethz.ch
[1] Geological Institute, ETH Zurich, 8092 Zürich, Switzerland
[2] Institute of Geophysics, ETH Zurich, 8093 Zürich, Switzerland

flows (e.g. Sletten et al. 2003), rockfalls (Lemcke 1992; Blikra et al. in press; Bussmann 2006) and shore collapses (e.g. Heim 1876, 1888, 1932; Kelts & Hsü 1980; Prior et al. 1984; Hsü & Kelts 1985; Siegenthaler & Sturm, 1991a, 1991b; Longva et. al 2003). Strong historic earthquakes left characteristic multiple mass-movement deposits at the lake/ocean floor (Shilts & Clague 1992; Schnellmann et al. 2002; Locat et al. 2003; Skinner & Bornhold 2003). Based on the fingerprints of historic events in "recent" sediments, similar prehistoric events can be recognized in older deposits (Schnellmann et al. 2002; Skinner & Bornhold 2003; Sletten et al. 2003).

Lake Lucerne and its surroundings are characterized by a high activity of both subaerial and subaqueous mass movements. Beside the direct threats caused by such events, at least three times in the last ~ 400 years, subaerial rockfalls or subaqueous slides have caused tsunamis and seiches in the lake. These incidents led to considerable damage along the shoreline (Bünti 1914; Billeter 1916; Cysat 1969; Huber 1980; Siegenthaler et al. 1987; Siegenthaler & Sturm 1991b). During the M_w ~ 6.2 earthquake in 1601 A.D. (Fäh et al. 2003), two subaerial rockfalls, various shore collapses and up to 4-m-high tsunami and seiche waves appeared in the lake (Cysat 1969; Schwarz-Zanetti et al. 2003). Consequently, the sediments in Lake Lucerne represent a suitable archive for characterizing the fingerprint of historic mass-movement and earthquake events and for extending the catalogue of such incidents to prehistoric times.

The aim of the study presented in this paper is: (1) to characterize and distinguish deposits related to subaqueous slides and subaerial rockfalls, (2) to establish a chronological catalogue of Late Glacial and Holocene mass-movement deposits in the Chrüztrichter and Vitznau basins of Lake Lucerne, (3) to identify and characterize hot spots with frequent past slide and rockfall activity, and (4) to recognize multiple mass-movement events, which were potentially triggered by strong prehistoric earthquakes.

2. Methods

In order to image the subsurface of the studied basins in quasi-3D, a grid of more than 300 km 3.5 kHz seismic lines (pinger source) was acquired in 2000 and 2001. As this study focuses on slope and base-of-slope processes, the line orientation was chosen perpendicular to the slopes rather than strictly parallel. The source/receiver was mounted on a cataraft that was pushed ahead by a vessel. DGPS-Positioning with a maximum error of ± 2 m guaranteed an accurate navigation. Processing of the digitally recorded data included a band-pass filter, an automatic gain control, a water-bottom mute and a spiking deconvolution. For conversion of two-way traveltime to water depth and sediment thickness, a constant velocity of 1500 ms^{-1} was used.

In 2000, eight Kullenberg-type gravity piston cores (Kelts et al. 1986), each 8–10 m-long, were retrieved from key locations in the Chrüztrichter and Vitznau basins. During a second coring campaign in 2002, the deeper subsurface (8–20 m) was

cored at two different sites by using an UWITEC percussion piston coring device.

Petrophysical properties of the sediments (P-wave velocity, gamma-ray density and magnetic susceptibility) were measured on whole cores with a GEOTEK Multi-Sensor Core Logger. After splitting, the cores were photographed and described macroscopically. Preparation and pretreatment of sample material for AMS ^{14}C dating was carried out in the ^{14}C laboratory of the Department of Geography at the University of Zurich. The dating itself was made using the tandem accelerator of the Institute of Particle Physics at ETH Zurich.

3. Study Area: Geological Setting and Historical Mass movement Activity

Lake Lucerne is a fjord-type lake of glacial origin with a total surface area of 116 km^2 (Fig. 1A). It is located in Central Switzerland at the northern alpine front and consists of seven steep-sided basins separated by subaqueous sills. Four major alpine rivers (Reuss, Muota, Engelberger Aa and Sarner Aa) drain a large part of the catchment (2124 km^2) and provide ~80% of the lakes total water supply (109 m^3/s). This study concentrates on the Chrüztrichter and Vitznau basins, which lack major active deltas and, as a consequence, show low sedimentation rates (Fig. 1A). The studied basins incorporate the alpine and the subalpine front, two major alpine thrusts separating (from S to N) Alpine Nappes, Subalpine Molasse and Plateau Molasse (Fig. 1A).

The southern shores of the studied basins are dominated by the steep Helvetic limestone cliffs of Bürgenstock Mountain. From the lake shore towards the top of Bürgenstock mountain the terrain raises about 700 m over a horizontal distance of 400 m. Rockfall deposits and talus debris are abundant at the base of these cliffs (Buxtorf 1918). During a historic rockfall close to Obermatt in 1964 approximately 70,000 m^3 of limestone fell into the lake. The induced wave was 10–15 m-high close to the impact and still caused considerable damage on the 3.5 km distant opposite lake shore (Huber 1980). Another rockfall at Bürgenstock occurred during the 1601 A.D. earthquake and contributed to huge water movements observed in the lake (Cysat 1969).

The northern shore of the Vitznau Basin is dominated by Rigi Mountain, which tectonically belongs to the Subalpine Molasse. The varying erosion resistance of individual Molasse beds results in a stepwise morphology. Parts of the steep conglomerate cliffs frequently break away, leading to relatively small rockfalls (e.g. Kanton Luzern 2006a, 2006b). Most rockfall deposits at the northern shore of Vitznau Basin occur between Riedsort and Vitznau (Fig. 1B), e.g. the remnants of a historic rockfall, which destroyed the therapeutic baths at Lützelau in 1661 (Kanton Luzern 2006b). Prehistoric deposits in the same region point towards at least one older and considerably larger event (Kanton Luzern 2006b). The process of this prehistoric incident was probably similar to the 1806 Goldau rockslide, which also took place in a subalpine Molasse setting
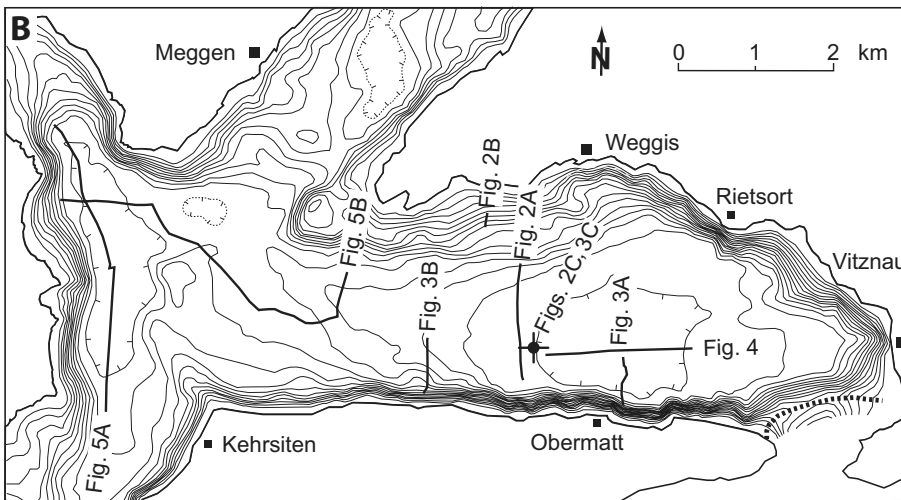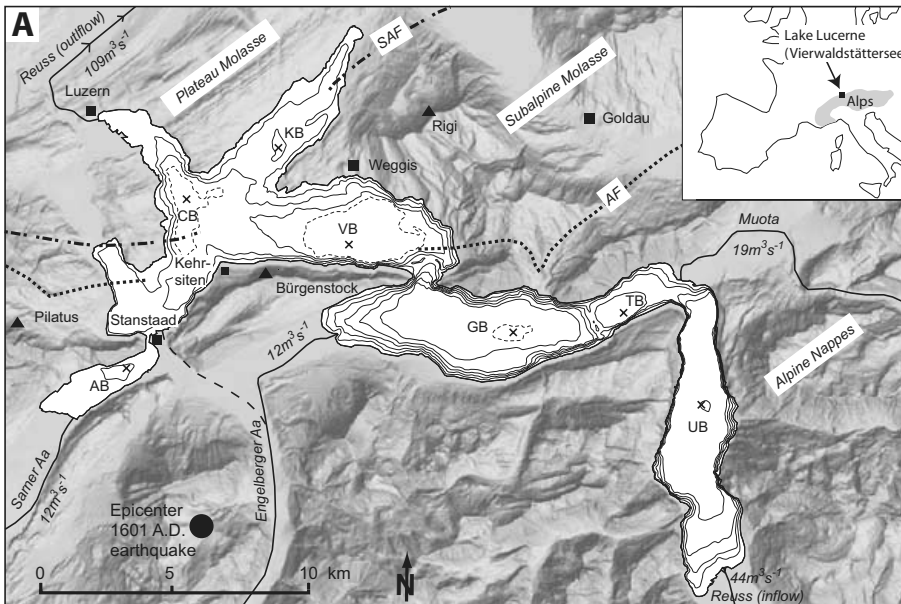
Fig. 1. A. Lake Lucerne and surroundings. The dotted and dashed-dotted lines mark the alpine front (AF) and the subalpine front (SAF), respectively. These two major thrusts separate the three main tectonic units of the area, which are, from north to south, the Plateau Molasse, the Subalpine Molasse and the Alpine Nappes (Helvetic Nappes and Penninic cliffs). The X's indicate the deepest points of the seven basins of the lake: Alpnach Basin (AB), Chrüztrichter Basin (CB), Gersau Basin (GB), Küssnacht Basin (KB), Treib Basin (TB), Uri Basin (UB) and Vitznau Basin (VB). Contour interval of the bathymetry is 40 m. Dotted lines contour 20 m intervals and aim to clarify the basin morphology. The epicenter of the 1601 A.D. earthquake was determined macroseismically with a location uncertainty of 20 km (Fäh, et al., 2003). B. Bathymetry of the studied basins and location of seismic lines and sediment cores shown in Figures 2–5. The bathymetry is based on the seismic data acquired during this study. Contour intervals of solid and dotted lines are 10 m and 5 m, respectively.

and involved thick conglomerate Bussmann 2006 beds sliding away on marly layers (e.g. Heim 1932; Kopp 1936).

Beside rockfalls and rockslides the northern shore of Vitznau basin has also faced destructive debris flows and shore collapses: In 1674, a debris flow triggered by a landslide (Gassrübi Landslide) above Vitznau damaged the southern part of the village (Kaufmann 1872; Zimmermann 1913; Lemcke 1992). A particularly destructive event took place in 1795 A.D., when a slow-moving subaerial landslide (Rubi Landslide) broke away above the village of Weggis. Thanks to detailed historical information including a map of the event, it is known that the event destroyed 28 houses and 15 barns and was over 300 m wide at the shore of the lake (Pfyffer 1795; Kanton Luzern 2006a). The debris flow triggered a sudden collapse of the lake shore, which induced a lowering of the lakebed by approximately 15 m. Shore collapses happened also during the 1601

A.D. earthquake (Cysat 1969). The most serious case described for Vitznau and Chrüztrichter basins affected the village of Vitznau, where a considerable piece of flat riparian land disappeared in the lake and large cracks opened in the ground, leading to the destruction of a mill and a sawmill.

4. Sedimentation in Chrüztrichter and Vitznau basin

Air gun reflection seismic profiles revealed a 117 m-thick, glacio-lacustrine infill in the central part of the Vitznau Basin (Finckh et al. 1984). The majority of these sediments were deposited in the Late Glacial period and only the uppermost 5 to 15 m are of Holocene age. Cores through the uppermost part of the Late Glacial sediments reveal thinly laminated light gray to yellowish mud with frequent intercalated graded turbidite beds of brown, gray and beige color. The Holocene sediments
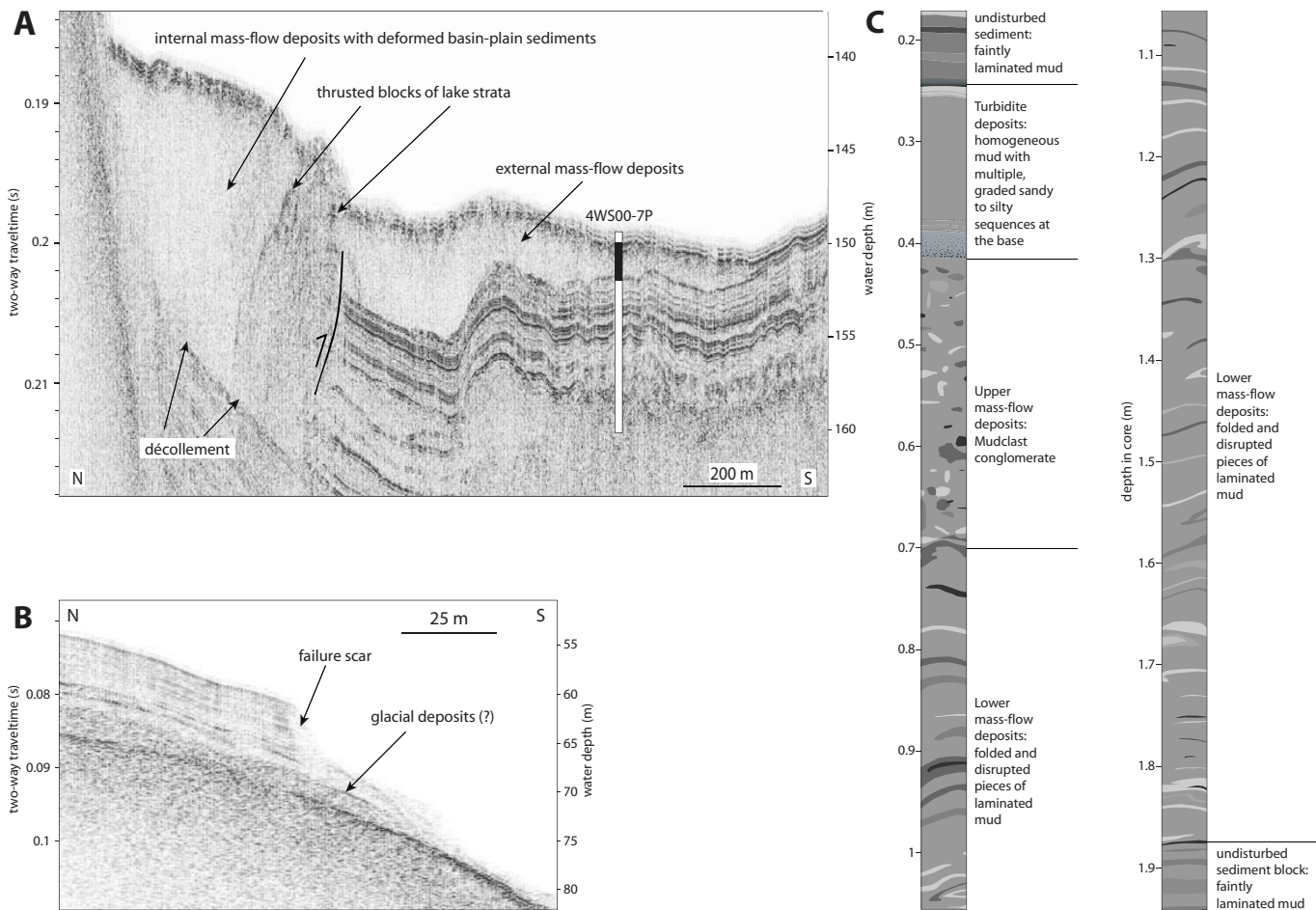
Fig. 2. Slide-evolved mass-flow deposits in Vitznau Basin. See Figure 1B for location of the seismic lines and the sediment core. A. Seismic profile across the basin fill of Vitznau Basin. B. Seismic line across the subaqueous slide scar related to the mass-flow deposit shown in Figure 2A. C. Sediment core (4WS00-7P, 0.18 – 1.93 m) through slide-evolved mass-flow deposits. The location of the core is indicated as vertical black bar on the seismic section in Figure 2A.

consist of faintly laminated, gray to brown mud with frequent organic-rich layers (mainly leafs and debris of land plants) and some intercalated graded turbidite beds. The uppermost sediment consists of biochemical varves (Sturm & Lotter 1995), which, in the deepest part of Vitznau Basin, are continuous since 1945 A.D. (Lemcke 1992). Between the Vitznau and the Chrüztrichter basins, the sedimentary characteristics gradually change, particularly the number and color of turbidite layers. Whereas most of the turbidite beds in the Vitznau Basin have a beige to yellowish color, dark brown turbidite beds dominate in the Chrüztrichter Basin.

In contrast to many other perialpine lakes in Switzerland, there is no evidence for considerably higher past lake levels in Lake Lucerne (Kopp 1938). Peat layers in boreholes at the shore, however, indicate up to 9 m lower lake levels in prehistoric times compared to today. This is supported by traces of prehistoric settlements in water depths of 6–8 m, which relate to a period between 6000 and 5400 cal. yr B.P. (Eberschweiler 2003). The most probably stepwise rise of the lake level since

that time is related to the growth of two opposing deltas in the outlet region near Lucerne (Kopp 1938). Since the foundation of the city of Lucerne at the beginning of the 13th century, lake level rose about 3–4 meters mainly due to man-made regulations of the outflow river.

Previous studies identified mass-flow deposits and exceptional turbidite beds in the subsurface of Lake Lucerne and related these deposits to historically-documented catastrophic events. Siegenthaler et al. (1991a) associate turbidite beds in the most internal and southern basin of Lake Lucerne (Urnersee) to historically documented floods, rockfalls and subaqueous slide events (both seismically and aseismically triggered). Hsü & Kelts (1985) detected a large mass-flow deposit in the subsurface of Vitznau Basin and interpreted it as the subaqueous continuation of the 1795 Rubi Landslide. Siegenthaler et al. (1987) proposed an alternative explanation for the same mass-flow deposit: Based on the peculiar characteristics of the thick turbidite bed directly overlying the mass-flow deposit, they associated the mass flow-turbidite sequence to
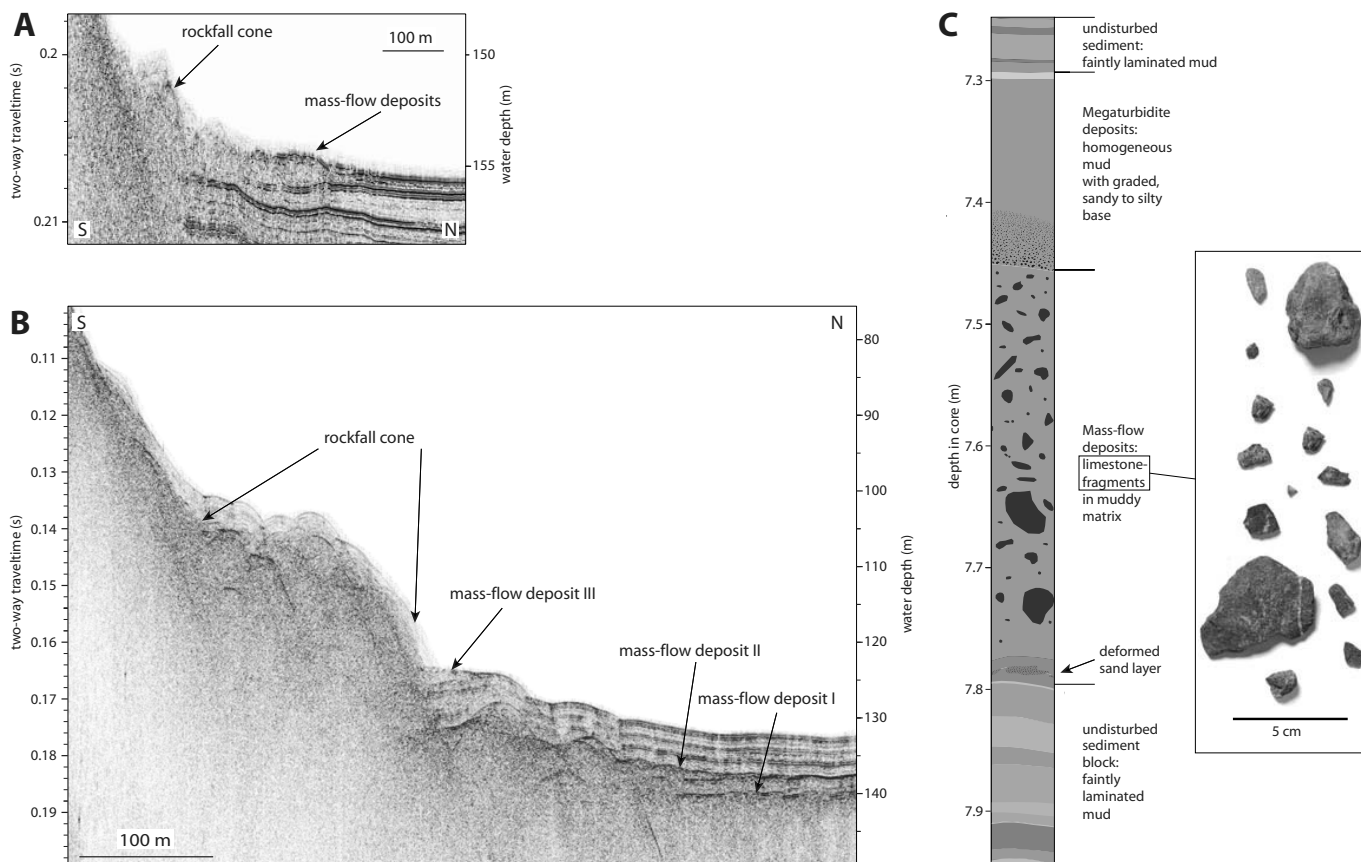
Fig. 3. Subaqueous rockfall cones and rockfall-evolved mass-flow deposits at the foot of Bürgenstock Mountain. See Figure 1B for location of the seismic lines and the sediment core. A. Seismic profile across the deposits related to the 1964 A.D. Obermatt rockfall. B. Stacked mass-flow deposits at the foot of a major rockfall cone. C. Sediment core (4WS00-7P, 7.27 – 7.93 m) through rockfall-evolved mass-flow deposits and photograph of rockfall-debris.

shore collapses and cyclic water movements chronicled in relation with the 1601 A.D. earthquake. This was confirmed by Lemcke (1992), who developed the first reliable age model for the sediments of the Vitznau Basin. With detailed mineralogical analyses and ^{137}Cs-dating, he could relate a characteristic bundle of beige layers and a gray turbidite bed to the 1679 A.D. Gassrübi Landslide and to the 1964 A.D. Obermatt Rockfall, respectively. This allowed calculation and down core extrapolation of the sedimentation rate and showed that the major mass-flow deposit identified by Hsü & Kelts (1985) relates to the 1601 A.D. earthquake and not to the 1795 Rubi Landslide.

5. Types of Mass-Movement Deposits

Unlike the undisturbed autochthonous background sediment, mass-movement deposits do not show a continuous acoustic layering and can therefore readily be recognized on seismic sections. Based on different geometries and seismic facies we distinguish between two different types of mass-movement deposits, which are described in the two following subchapters.

5.1 Mass-flow deposits

The most common type of mass-movement deposits identified in the study area image as basinwards-thinning bodies with distinct distal terminations, a chaotic or chaotic-to-transparent seismic facies and hummocky to relatively smooth top surfaces (Figs 2–4). Such geometries and seismic facies are typical characteristics of mass-flow deposits (e.g. Nardin et al. 1979; Prior et al. 1984; Mulder & Cochonat 1996).

In distal areas, the mass-flow deposits are relatively thin and overlay undisturbed or only superficially disturbed sediment with a continuous acoustic layering (Fig. 2A). Close to the slope break, the mass-flow deposits are thicker and the chaotic-to-transparent facies reaches deeper, indicating deformation of the overridden basin-plain sediment. The lateral boundary between undisturbed and deformed basin-plain sediment is marked by an abrupt lateral termination of continuous reflections (Fig. 2A). Deformation zones reach thicknesses >10 m and often show clear basal décollement surfaces. In most cases, the mass-flow deposits in the strict sense and the deformed basin-plain sediments cannot be distinguished on seismic sections, due to a similar seismic facies. However, close
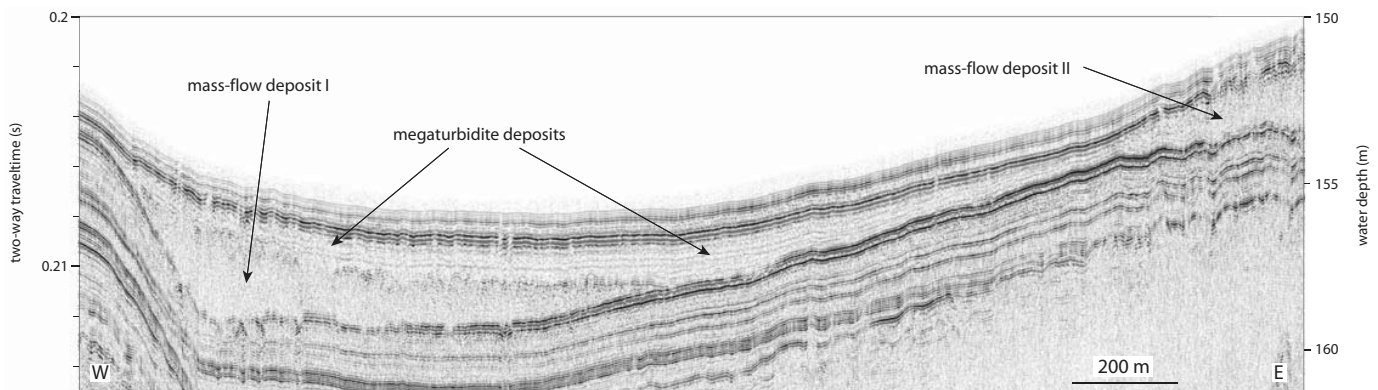
Fig. 4. Megaturbidite in Vitznau Basin directly overlaying two coeval mass-flow deposits. Note the characteristic, almost transparent seismic facies and the ponding geometry of the megaturbidite. See Figure 1B for location of the seismic line.

to the deformation front, it is sometimes possible to recognize thrusted blocks of acoustically layered basin-plain sediment (Fig. 2A). The deep-reaching deformation of the marginal basin fill is regarded as the result of an adjustment of the basin-plain sediments to the increased static and dynamic loading during mass-flow deposition (Schnellmann et al. 2005).

Failure scars reaching heights >6 m have been identified on many seismic profiles throughout the study area, most of them on steepening-downwards slopes with 10–20° inclination. In most cases, the whole acoustically-lavered drape is removed below fresh slide scars and the acoustic bedrock is exposed. As no attempts have been made in this study to core the glide plane, it remains unclear whether the acoustic bedrock represents glacial sediments or molasse. However, in some cases, a thin layer of sediments with a high-amplitude chaotic-to-transparent seismic facies overlies the acoustic bedrock (Fig. 2B). Here the glide plain most likely consists of glacial deposits.

Many of the mass-flow deposits in the basin plain can be related to failure scars on the slope above and are therefore regarded as slide-evolved. Coring of such slide-evolved mass-flow deposits revealed deformed lake sediment. In the upper part, the sediment is heavily deformed and builds up a matrix-supported mud-clast conglomerate. In the lower part, deformation is much more localized and larger pieces of internally undeformed lake strata occur (Fig. 2C).

Other mass-flow deposits relate to rockfall cones (Fig. 3), which appear at the foot of steep cliffs and building up positive reliefs with irregular hummocky top surfaces. The cones are generally not penetrated by the high-resolution seismic signal. In the superfical part discontinuous high-amplitude reflections and diffractions are abundant and probably relate to blocky rock debris. At the foot of such cones, wedge-shaped mass-flow deposits with basinwards smoothing top surface and a chaotic- to high-amplitude chaotic seismic facies occur. The 1964 event produced a relatively small rockfall cone with a single mass-flow deposit (Fig. 3A). Figure 3B shows a considerably larger rockfall cone associated with three mass-flow deposits at different stratigraphic levels, indicating repeated

rockfall activity at the same location. The two lower deposits (labeled mass-flow deposits I & II in Fig. 3B) are characterized by a high-amplitude-chaotic seismic facies, a common feature of large rockfall-evolved mass-flow deposits. The uppermost deposit (mass-flow deposit III) is of little extent and thickness and shows a chaotic-to-transparent rather than a high-amplitude-chaotic seismic facies. This relatively small deposit may result from the sliding of lake sediment deposited on the slopes of the rockfall cone and is, therefore, not necessarily related to a rockfall event. Cores through rockfall-evolved deposits revealed a breccia of mud clasts and angular limestone fragments (Fig. 3C). Such rock fragments are most probably the reason for the higher amplitude of the seismic facies of rockfall-evolved compared to slide-evolved mass-flow deposits.

5.2 Megaturbidites

The mass-flow deposits are often directly overlain by a second, clearly different type of mass-movement deposits, which is characterized by a ponding geometry, an almost transparent seismic facies, a smooth top surface and maximum thicknesses reaching ~2 m. This geometry and acoustic signature is typical for thick, extensive turbidite deposits, which generally result from large mass flows (Bouma 1987).

Figure 2C shows a core through a complex turbidite related to the 1601 A.D. earthquake. It directly overlies a mass-flow deposit and is characterized by a multiple-graded sandy base, a 10 cm thick central part consisting of homogeneous medium gray mud and a light gray top. This complex turbidite is interpreted as result of multiple sliding and related cyclic water movements in 1601 A.D. Turbidites related to rockfalls generally show a particularly thick sandy base (Fig. 3C), which thins out to thin sand or silt layers towards more distal positions.

Although turbidites associate to most of the larger mass-flows in the study area, many of them are too small to be resolved on seismic sections. Only the turbidite beds with bed thickness >15–20 cm could be mapped out in this study. In the following, we use the term "megaturbidite" for such 'map-
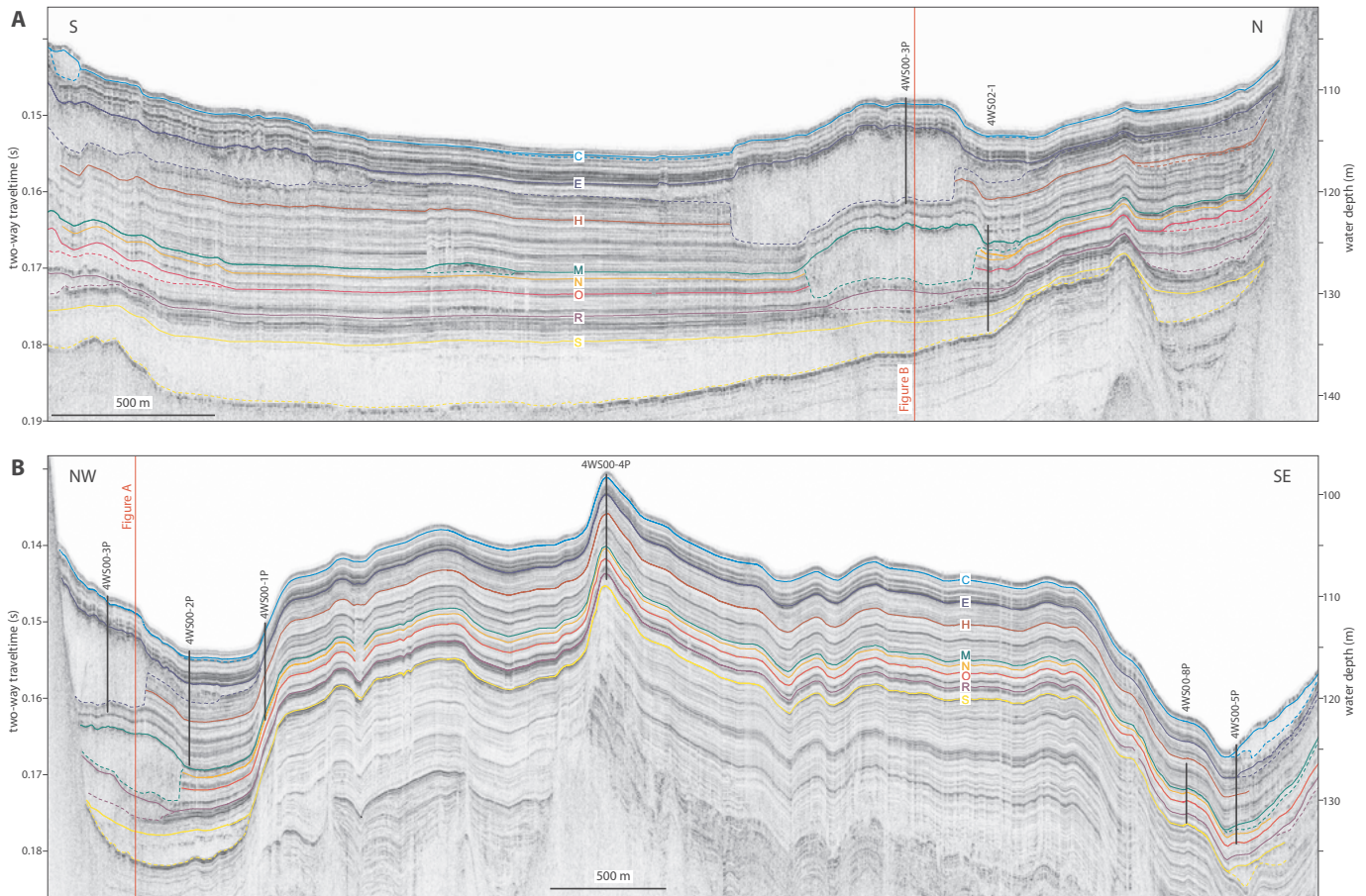
Fig. 5. Mapping of event horizons. A and B show two composite seismic lines across the western part of the study area. See Figure 1B for location of the seismic profiles. The crossing between the two lines is indicated by solid vertical red lines. Different-colored solid lines mark seismic stratigraphic horizons relating to the top of mass-flow deposits and megaturbidites. Note that some horizons lie directly on top of more than one mass-flow deposit indicating synchronous deposition. Dashed colored lines mark the base of megaturbites, mass-flow deposits and deformed basin-plain sediment. Coring sites are indicated with bold vertical black lines.

pable' turbidites, which generally relate to major mass movements and the potentially related tsunami and seiche waves.

A somewhat untypical megaturbidite is outlined in yellow colors in Figure 5. Its thickness of up to 6 m is exceptional and, compared to all other identified megaturbidites, its seismic facies is less transparent and includes short-range continuous reflections. Nevertheless, it shows a ponding geometry. A core (core 4WS02-1), which, according to the seismic-to-core correlation, did not quite reach the base of these deposits, revealed a more than 1.3 m-thick, fining upward unit overlain by 40 cm of ungraded, homogeneous sediment. The possible origins of this unusual turbidite will be discussed in chapter 7.3.

6. Catalogue of Past Mass-Movement Deposits

6.1. Seismic stratigrapic mapping of event horizons

With the help of a dense grid of more than 300 km high-resolution seismic lines, we identified and mapped out 91 mass-flow deposits and 6 megaturbidites (Figs 5, 6). For establishing a chronology of past mass movements, the top of each mass-flow and megaturbidite deposit was determined and tied to a specific seismic stratigraphic horizon (Fig. 5). The exact seismic stratigraphic position of a mass-movement deposit can best be determined at the toe or pinch-out point of a deposit. In the internal part of mass-flow deposits it is often difficult to clearly identify the top due to the presence of hummocky mass-flow surfaces. The seismic stratigraphic horizons related to specific mass-movement deposits were mapped throughout the lake, in order to recognize synchronous deposits and to allocate them to the same "event horizon" (= seismic stratigraphic horizon related to at least one mass-movement deposit).

In this way, 19 individual event horizons were identified and labeled as Event A (young) to Event S (old) according to stratigraphy. The distribution of mass-movement deposits related to each of the event horizons are shown in Figure 6. Each of the event horizons comprises between 1 and 19 mass-flow and megaturbidite deposits.
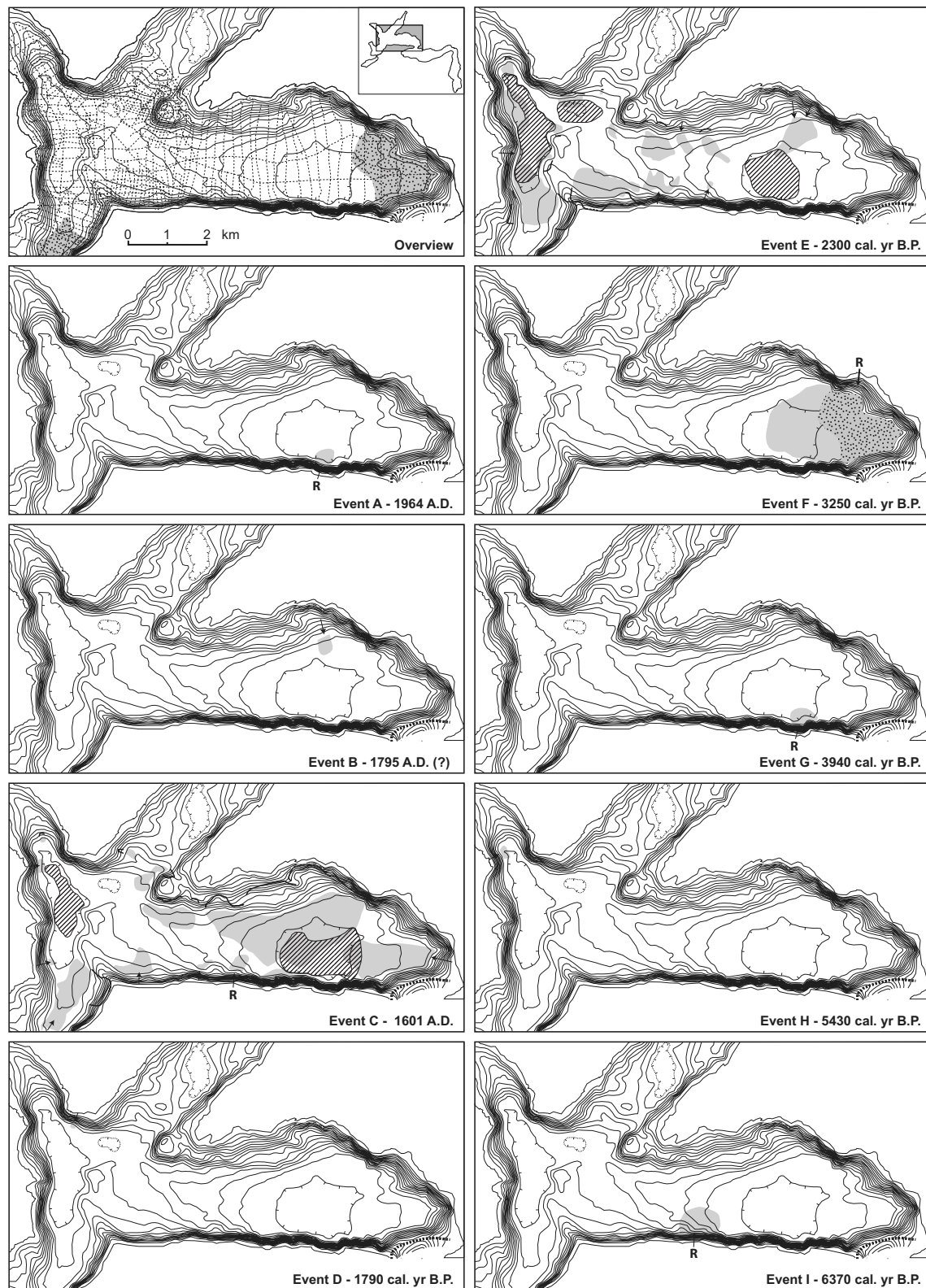
Fig. 6. Catalogue of mass-movement deposits in the subsurface of Lake Lucerne. The upper left panel shows the seismic survey grid, which was used for mapping and correlating the mass-movement deposits. The other panels show the areal distribution of events A to S. Zones with limited seismic penetration are indicated by dotted surfaces. Gray and hatched surfaces mark mass-flow deposits and megaturbidites, respectively. Bold solid lines delineate slide scars. Mass-flow deposits interpreted as rockfall-evolved are indicated by "R". For dating procedure and age ranges, see Tables 1 and 2.

Event J - 7750 cal. yr B.P.

Event O - 11,730 cal. yr B.P.

Event K - 8010 cal. yr B.P.

Event P - 11,930 cal. yr B.P.

Event L - 9310 cal. yr B.P.

Event Q - 12,930 cal. yr B.P.

Event M - 9870 cal. yr B.P.

Event R - 13,710 cal. yr B.P.

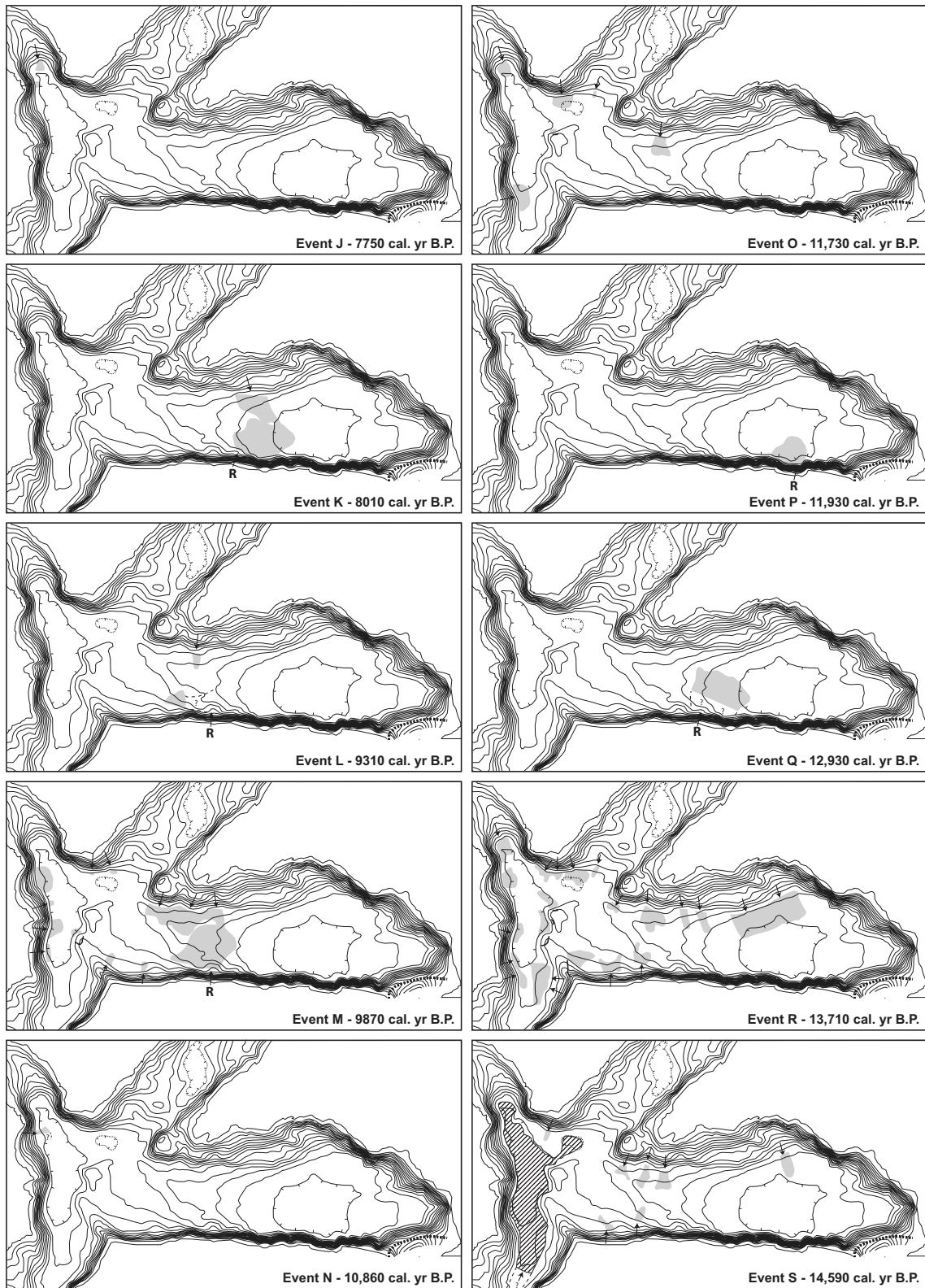Event N - 10,860 cal. yr B.P.

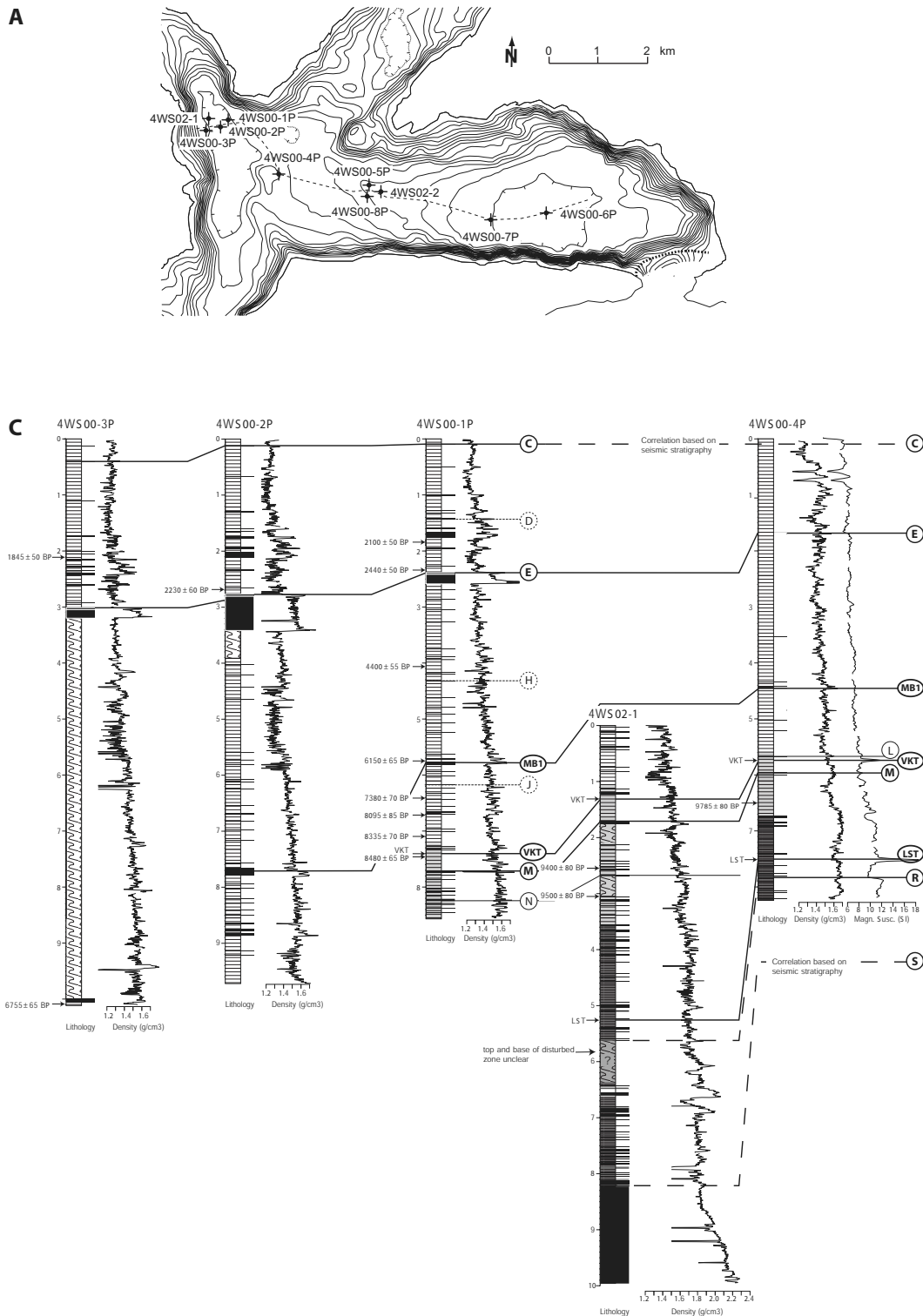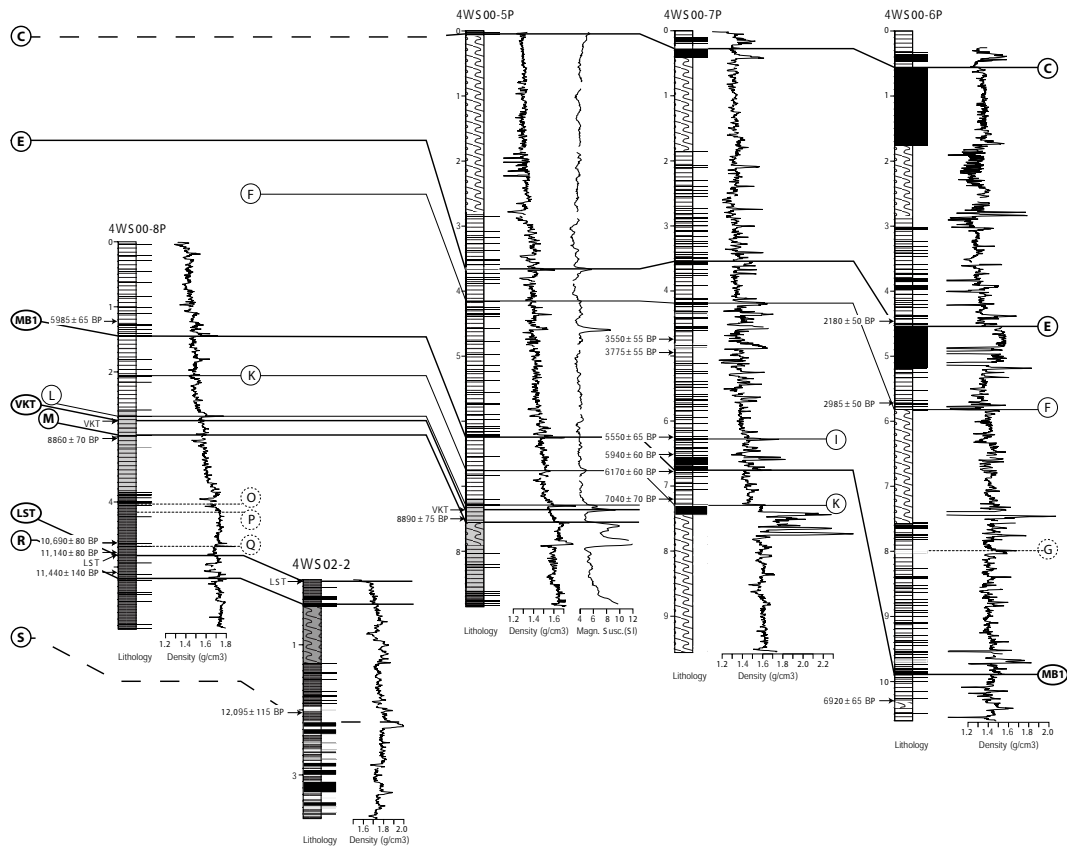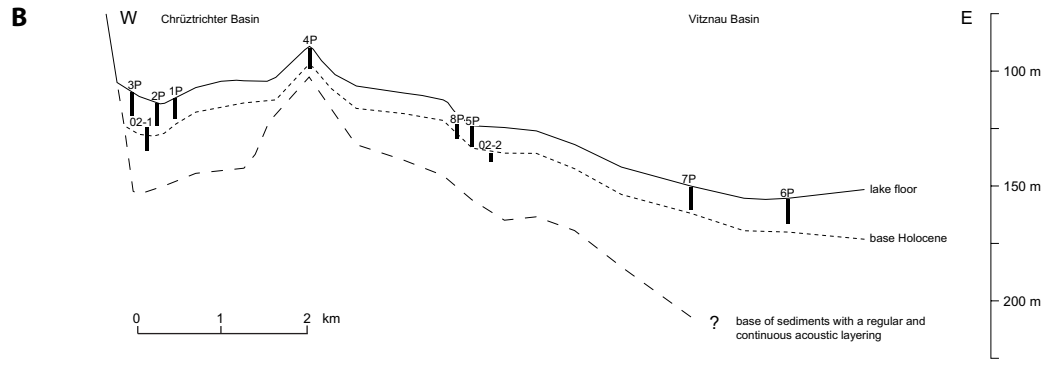Event S - 14,590 cal. yr B.P.

Fig. 6. part 2

Fig. 7. Core-to-core correlation along an E-W transect. A. Location of coring sites. B. Cross section across the study area with coring sites indicated by vertical black bars. C. Core-to-core correlation based on lithology, density and magnetic susceptibility. Solid lines delineate core-to-core correlation of mass-movement horizons and other marker beds. Uncertain correlations are indicated with dashed lines. Dotted horizontal lines show the litho-stratigraphic positions of event horizons, which did not leave characteristic deposits like deformed beds or turbidites in the available cores. The lithostratigraphic positions of such events are solely based on seismic-to-core correlation (see text for further explanation). Note the two peaks in the magnetic susceptibility log of core 4WS00-4P at 5.75 m and 7.52 m, which relate to the Vasset Killian (VKT) and to the Laacher See Tephra (LST), respectively. Markerbed MB1 represents a characteristic sequence of closely spaced turbidites, which was used for core-to-core correlation.

B

W Chrüztrichter Basin   Vitznau Basin   E

— 100 m

— 150 m

— 200 m

lake floor

base Holocene

? base of sediments with a regular and continuous acoustic layering

0   1   2 km

4WS 00-5P
4WS 00-7P
4WS 00-6P
4WS 00-8P
4WS 02-2

faintly laminated gray mud with intercalated turbidites (indicated by black bars) and frequent organic material

laminated medium to light gray mud with intercalated turbidites (indicated by black bars) and little organic material

very thinly laminated light gray to yellowish mud with frequent intercalated turbidites (indicated by black bars)

deformed sediment beds comprising highly reworked mud clast conglomerates as well as larger blocks of internally undisturbed blocks of lacustrine strata
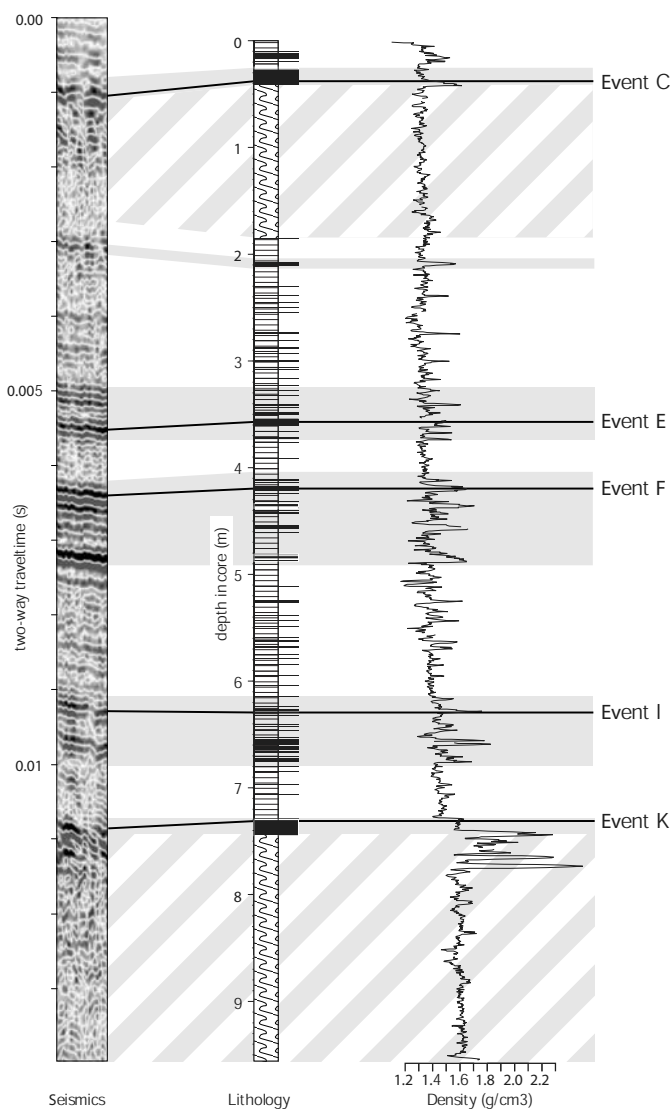
Fig. 7. part 2

Fig. 8. Seismic-to-core correlation (Core 4WS00-7P; for position see Fig. 7A). Gray bars highlight the correlation between high-reflective zones in the seismic data, high turbidite frequency and distinct changes of the gamma-ray density. Hatched zones indicate acoustically chaotic-to-transparent areas on the seismic profile and corresponding deformation intervals in the sediment core. Solid lines delineate the correlation between seismic stratigraphic event horizons and specific lithological beds.

The catalogue of past mass-movement activity shown in Figure 6 is not complete because: (1) only the youngest deposits were mapped out in the very eastern part of Vitznau Basin and in the southern part of Chrüztrichter Basin due to limited penetration of the seismic signal, (2) relatively small and/or old mass-movement deposits may not have been recognized due to reworking and deformation by younger and larger events, and (3) some, mostly small, mass-movement deposits could not be included in the mass-movement event catalogue due to the lack of clear tops or pinch out points.

6.2. Coring of the event horizons

To date the prehistoric event horizons, 10 sediment cores reaching subsurface depths up to 20 m were retrieved from key locations, which were chosen based on the seismic data (Figs 5, 7A, B). Mass-flow and megaturbidite deposits related to the most prominent event horizons (Fig. 6 – Events C, E, M, R, S) were cored in both, the Chrüztrichter and Vitznau Basins in order to accurately date these deposits and to check the synchronicity of mass-flow deposits relating to specific seismic stratigraphic event horizons by core-to-core correlation. To allow accurate correlation and to overcome changing sedimentary characteristics between Vitznau and Chrüztrichter Basins, the coring sites were chosen along an E-W transect and the maximum distance between different coring sites was kept small (Figs 7A, B). In cores, the limits between mass-flow deposits and autochthonous sediment are difficult to identify, as transported blocks of former strata often remain internally undisturbed (Schnellmann et al. 2005). Hence, along with cores through mass-flow deposits, cores from nearby undisturbed sites were retrieved. Correlation between the two cores generally allowed identification of top and base of the mass-flow deposits.

Comparison of the seismic reflection patterns with lithological and gamma-ray density logs of the cores enables an accurate seismic-to-core correlation (Fig. 8). Reflection patterns characterized by high-amplitude reflections were matched with pronounced density changes, which typically relate to coarse and dense turbidite beds. Zones with a chaotic-to-transparent seismic facies were correlated to deformed sediment beds. For the majority of the seismic stratigraphic event horizons (Fig. 6 – Events C, E, F, I, K, L, M, N, R, S), the exact litho-stratigraphic position could be determined due to characteristic layers, such as deformed deposits, (mega)turbidite beds or sand layers. Other events identified on the seismic data, however, did not leave direct traces at the coring sites. The litho-stratigraphic positions of such event horizons (Fig. 6 – Events D, G, H, J, O, P, Q) have been determined from their relative position between two known event horizons.

Correlation between neighboring cores was achieved by comparing both petrophysical properties and visual characteristics (Fig. 7C). In this way, and because of the relatively small maximum distance between the coring sites, a good core-to-core correlation was established. The following marker beds were traced throughout the basins and coring sites: (1) the mass-flow and (mega)turbidite beds related to Event E, (2) a characteristic sequence of closely spaced turbidite deposits (MB1), (3) The Boreal Vasset-Killian Tephra (VKT), (4) the mass-flow and turbidite beds related to Event M, and (5) the Allerød Laacher See Tephra (LST). The VKT and LST Tephras origin from volcanic eruptions in the Massive Central, Central France, and the Eifel, Western Germany, respectively. Both tephra-layers have been identified in several lakes in Switzerland (Hajdas et al. 1993; Shotyk et al. 1998) and SW-Germany (Merkt 1971; Mayer & Schwark 1999) and show dis-

Table 1. Calibration of radiocarbon ages

core nr	depth in core (cm)	sample nr	AMS ^{14}C age *	calibrated age (cal. yr B.P.) †	∂13C (‰)	material
4WS00-1P	234.1	UZ-4571	2440 ± 50	2352–2711	-20.6 ± 1.2	leaf remains
4WS00-2P	268.5	UZ-4572	2230 ± 60	2069–2349	-22.3 ± 1.2	leaf remains
4WS00-6P	446	UZ-4573	2180 ± 50	2044–2329	-23 ± 1.2	leaf remains
4WS00-6P	571.6	UZ-4574	2985 ± 50	2996–3332	-20.6 ± 1.2	leaf remains
4WS00-6P	1029.5	UZ-4575	6920 ± 65	7614–7925	-20.6 ± 1.2	leaf remains
4WS00-1P	746.1	UZ-4585	8480 ± 65	9300–9552	-21.1 ± 1.2	wood
4WS00-8P	124.6	UZ-4643	5985 ± 65	6667–6986	-13.3 ± 1.2	leaf remains
4WS00-8P	302.5	UZ-4644	8860 ± 70	9702–10,183	-24.9 ± 1.2	wood
4WS00-8P	508.3	UZ-4645	11,440 ± 140	13,025–13,829	-26.4 ± 1.2	leaf remains
4WS00-8P	477.6	UZ-4646	11,140 ± 80	12,692–13,736	-6.6 ± 1.2	wood
4WS00-8P	462.9	UZ-4647	10,690 ± 80	12,347–12,978	-21.7 ± 1.2	wood
4WS00-4P	650	UZ-4789	9785 ± 80	10,764–11,546	-26.2 ± 1.2	leaf remains
4WS00-8P	214.7	UZ-4790	7575 ± 75	8184–8536	-26.1 ± 1.2	leaf remains
4WS00-7P	720	UZ-4791	7040 ± 70	7695–7969	-25.2 ± 1.2	nut
4WS00-8P	169.4	UZ-4792	6705 ± 65	7437–7670	-26.9 ± 1.2	leaf remains
4WS00-5P	750.1	UZ-4793	8890 ± 75	9724–10,207	-24.7 ± 1.2	leaf remains
4WS00-7P	624.8	UZ-4794	5550 ± 65	6200–6472	-27.1 ± 1.2	leaf remains
4WS02-2	204	UZ-4840	12,095 ± 115	13,662–15,332	-21.5 ± 1.2	wood
4WS02-1	254.7	UZ-4841	9400 ± 80	10,289–11,068	-24.1 ± 1.2	leaf remains
4WS02-1	305.1	UZ-4842	9500 ± 80	10,560–11,113	-26.3 ± 1.2	wood
4WS00-3P	1008.6	UZ-4901	6755 ± 65	7480–7719	-22.4 ± 1.2	leaf remains
4WS00-1P	574.9	UZ-4949	6150 ± 65	6806–7233	-21.7 ± 1.2	wood
4WS00-1P	671.4	UZ-4950	8095 ± 85	8653–9395	-22.0 ± 1.2	leaf remains
4WS00-1P	641.1	UZ-4951	7380 ± 70	8025–8347	-24.7 ± 1.2	leaf remains
4WS00-1P	709.6	UZ-4952	8335 ± 70	9092–9516	-24.9 ± 1.2	wood
4WS00-1P	184.3	UZ-5038	2100 ± 50	1931–2300	-28.4 ± 1.2	leaf remains
4WS00-1P	406.3	UZ-5039	4400 ± 55	4848–5279	-25.2 ± 1.2	leaf remains
4WS00-3P	211.8	UZ-5040	1845 ± 50	1627–1916	-21.7 ± 1.2	wood
4WS00-7P	651.6	UZ-5041	5940 ± 60	6572–6934	-26.0 ± 1.2	leaf remains
4WS00-7P	677.3	UZ-5042	6170 ± 60	6894–7239	-27.5 ± 1.2	leaf remains
4WS00-7P	474.1	UZ-5043	3550 ± 55	3688–3980	-25.8 ± 1.2	wood
4WS00-7P	494.6	UZ-5044	3775 ± 55	3932–4352	-23.7 ± 1.2	leaf remains
VKT §		Tephra	8230 ± 140	8775–9526		
LST #		Tephra	11,230 ± 40	13,003–13,755		

* Preparation and pretreatment of sample material for radiocarbon dating was carried out by the ^{14}C laboratory of the Department of Geography at the University of Zurich (GIUZ). The dating itself was done by AMS (accelerator mass spectrometry) with the tandem accelerator of the Institute of Particle Physics at ETH Zurich. † Calibration (2 sigma range) was carried out with CALIB 4.4 software (Stuiver and Reimer, 1993). § Vasset Killian Tephra (VKT), radiocarbon dated by Hajdas et al. (1993). # Laacher See Tephra (LST), radiocarbon dated by Hajdas et al. (1995).

tinct peaks in the magnetic susceptibility curves of several Lake Lucerne cores (see core 4WS00-4P in Fig.7 for a typical example). For sediments older than the lower tephra layer, correlation between the basinal core 4WS02-1 and the cores 4WS00-4P and 4WS02-2, which were retrieved further away from the depocenters, could not be established. This is most probably due to the enhanced focusing of Late Glacial sedimentation in the basin centers, which results in large differences in both, sedimentation rates and sediment characteristics from basinal to more elevated environments.

6.3. Dating of the event horizons

The three youngest event horizons (Fig. 6 – Events A, B, C) all occurred in historical times. Events A and C have already been identified and dated in earlier studies and relate to the 1964 A.D. Obermatt rockfall and the 1601 A.D. earthquake, respectively (Siegenthaler et al. 1987; Lemcke 1992). Event horizon B lies stratigraphically between these two events and comprises only a single mass-flow deposit, which is located offshore the village of Weggis. Based on high-resolution seismics and core analysis, Zwyer (2006) showed that this deposid results from a subaqueous continuation of the 1795 A.D. Rubi landslide.

Thirty-two samples from various depths and cores were collected for AMS-radiocarbon dating (Table 1). To minimize the risk of dating reworked samples, terrestrial leaf remains were the preferred sample material. However, particularly in Late Glacial deposits, where organic material is scarce, small fragments of wood were also used for dating. Further age con-

Table 2. Dating of prehistoric event horizons

horizon name	sample nr	calibrated age*	offset (cm) †	sed.rate (cm/a)	horizon age sample*	overlap age of closest samples*	center of overlap *§
D	UZ-5040	1627–1916	1.9	0.11	1644–1933	1644–1933	1790
E	UZ-4571	2352 – 2711	4.3	0.08	2406– 2765	#	#
	UZ-4572	2069–2349	8.8	0.08	2179– 2459		
	UZ-4573	2044–2329	6	0.07	2130– 2415	2179–2415	2300
F	UZ-4574	2996–3332	6	0.07	3082– 3418	3082–3418	3250
G	UZ-5043	3688–3980	5.3	0.06	3776–4068		
	UZ-5044	3932–4352	-7.8	0.06	3802–4222	3802–4068	3940
H	UZ-5039	4848–5279	25.4	0.07	5211–5642	5211–5642	5430
I	UZ-4794	6200–6472	1.8	0.06	6230–6502		
	UZ-5041	6572–6934 -	19.9	0.06	6240–6602	6240–6502	6370
J	UZ-4949	6806–7233	36.8	0.06	7419–7846		
	UZ-4951	8025–8347	-22.3	0.06	7653–7975	7653–7846	7750
K	UZ-4791	7695–7969	9.1	0.05	7877–8151	7877–8151	8010
L	VKT	8775–9526	-6.8	0.05	8639–9390		
	UZ-4585	9300–9552	-10.1	0.05	9098–9350		
	UZ-4793	9724–10,207	-23	0.05	9264–9747		
	UZ-4644	9702–10,183	-32.3	0.05	9056–9537	9264–9350	9310
M	VKT	8775–9526	21.3	0.05	9201–9952		
	UZ-4585	9300–9552	18	0.05	9660–9912		
	UZ-4793	9724–10,207	5.1	0.05	9826–10,309		
	UZ-4644	9702–10,183 -	4.2	0.05	9618–10,099	9826–9912	9870
N	UZ-4841	10,289–11,068	9.3	0.06	10,444–11,223		
	UZ-4842	10,560–11,113	-4.3	0.06	10,488–11,041	10,488–11,223	10,860
O	UZ-4789	10,764–11,546	42.7	0.06	11,476–12,258		
	UZ-4647	12,347–12,978	-59.1	0.06	11,362–11,993	11,476–11,993	11,730
P	UZ-4789	10,764–11,546	54.7	0.06	11,676–12,458		
	UZ-4647	12,347–12,978	-47.1	0.06	11562–12,193	11,676–12,193	11,930
Q	UZ-4647	12,347–12,978	4.8	0.06	12,427–13,058		
	UZ-4646	12,692–13,736	-8.1	0.06	12,557–13,601		
	LST	13,003–13,755	-12.2	0.06	12,800–13,552	12,800–13,058	12,930
R	UZ-4647	12,347–12,978	51.6	0.06	13,207–13,838		
	UZ-4646	12,692–13,736	38.7	0.06	13,337–14,381		
	LST	13,003–13,755	34.6	0.06	13,580–14,332		
	UZ-4645	13,025–13,829	8	0.06	13,158–13,962	13,580–13,838	13,710
S	UZ-12095	13,662–15,332	13.8	0.15	13,754–15,424	13,754–15,424	14,590

* Ages in cal. yr B.P. † Position of the dated sample relative to the event horizon. § Ages are rounded to the decade. # Sample UZ-4571 is not included in the determination of the horizon age due to its anomalous age range (reworking?).

straints arose from the two tephra layers, which have been radiocarbon dated to 8230 ± 140 B.P. (VKT; Hajdas et al. 1993) and 11,230 ± 40 ^{14}C yrs B.P. (LST; Hajdas et al. 1995) in Soppensee, a small lake 20 km SW of Lucerne.

The ^{14}C-ages were transferred to calendar years (2s-range) with the Calib 4.3 software (Table 1; Stuiver & Reimer 1993). For dating an individual event horizon the lithostratigraphically closest 1-4 ^{14}C-ages were selected. The error introduced by the offset between the lithostratigraphic position of ^{14}C-age and event horizon was corrected using the estimated sedimentation rates applied to the sample-horizon offset (Table 2). In this way, for each of the 1-4 selected samples, an age range for the event horizon was calculated. Subsequently, the overlap of the obtained age-ranges and its center was determined. The same procedure was repeated for each of the event horizons.

7. Spatial and Temporal Distribution of Past Mass-Movement Activity

7.1. Subaqueous sliding

In order to identify subaqueous slopes, which are particularly susceptible to sliding, all failure scars and all non-rockfall evolved mass-flow deposits were superpositioned (Fig. 9A). The identified scars occur on steepening-downward sections of marginal slopes or subaqueous hills with at least partial inclinations >10° (Fig. 9). Stacked mass-flow deposits at the foot of slopes with distinct slide scars indicate repeated sliding on the same slope.

The surface covered by individual mass-flow deposits ranges from <0.01 km² to >6 km². Transported volumes are difficult to calculate, as slope material and reworked basin-

plain sediment often cannot be distinguished on seismic sections. Estimates of the volume transported by the two biggest mass-flow deposits revealed more than 10 million m³. The majority of the thick and extensive non-rockfall-evolved mass-flow deposits occur at the foot of slopes with inclinations of 10–20°, while only a few small mass-flow deposits are present below slopes steeper than 25° (Fig. 9). It seems that slopes with inclinations <10° are essentially stable and slopes with inclinations >25° are too steep to accumulate the sediment volumes needed for major sliding. The "Weggis Slide", one of the largest events in the study area (Fig. 6 – Event C), was triggered in an area with slope inclinations >10° before eroding flatter zones along its path. Once a slide is initiated, it is thus capable of eroding flatter slopes and thereby gaining volume.

Whereas the slide locations remain more or less the same from Late Glacial to Holocene times, the size of the Late Holocene mass-flow deposits tends to be larger compared to their older counterparts (Fig. 6). This is interpreted as a result of limited sediment deposition on the subaqueous slopes in Late Glacial times due to underflow-dominated sedimentation and limited productivity.

7.2. Rockfalls

Rockfall deposits occur along three zones in the southern and in the northeastern parts of Vitznau Basin. The location of the three rockfall cones and the corresponding number of rockfall-incidents (number of rockfall-evolved mass-flow deposits) is indicated for each of the three locations in Figure 9A. These are minimum numbers, as rockfall events can heavily rework the basin-plain sediment and thereby destroy traces of older events. In the rockfall zone on the northern shore of Vitznau basin, the lake sediments older than the major rockfall Event F (3250 cal. yr B.P.) cannot be imaged with the seismic data due to reworking and gas-blanking.

Our data indicate a higher rockfall activity at the northern face of Bürgenstock before 6000 cal. yr B.P. Later, both the number of rockfall events and the size of rockfall-evolved mass-flow deposits decreased. There is no indication of a persistent migration of the instable zone and the related rockfall activity along the cliff of Bürgenstock Mountain.

As the southern shore of the Vitznau Basin is scarcely populated, the major hazard related to such events arises from rockfall-induced waves. Such waves particularly affect the northern shore of Vitznau Basin, as observed during the 1964 A.D. Obermatt rockfall. Most of the prehistoric rockfalls identified in this study included larger volumes than this event. As the height of rockfall-generated waves is largely related to the volume of the displaced mass (Huber 1980; Vischer 1986), the waves generated by some of the prehistoric events may have been considerably larger than the historical example. However, the generation of waves by rockfalls is complex, and the shape and height of such waves also depend on many other parameters, such as shape and air content of the impacting mass, pathway-inclination and height of fall (Huber 1980; Fritz 2002).

7.3. Megaturbidites

The late Holocene multiple mass-movement events (Fig. 6; Events C, E) are associated with large megaturbidites. Minor turbidites have also been identified in relation to other events (Fig. 7 – Events F, I, K, L, M, N, R). However, due to their small size, these minor turbidites can not be seen on seismic sections, but only in cores. The following factors may be responsible for the high amount of resuspension and the build-up of thick megaturbidites related to the Events C and E: (1) the relatively large size and number of involved mass flows, (2) the existence and considerable size of slide-induced tsunami and seiche waves (Siegenthaler et al. 1987; Schnellmann et al. 2002), which potentially resuspend sediments from the lake floor (Siegenthaler et al. 1987; Chapron et al. 1999) and (3) the presumably high remobilization potential of the Late Holocene sediment.

As outlined in chapter 5.2, the large megaturbidite associated with Event S shows a seismic facies, which is less transparent and includes short-range continuous reflections. Although the base of the megaturbidite has not been reached, the coring indicates a much thicker graded sequence (Fig. 7 – core 4WS02-1) and a higher sand content compared to the other megaturbidites observed in this study. The lateral thickness distribution of the event indicates transport from the region of Stansstaad, where a paleodelta indicates a temporal drainage of Engelberger Aa River towards Chrüztrichter basin (Fig. 1). Transport direction and lateral sediment distribution could be explained by a delta collapse. Alternatively a catastrophic flooding in the catchment, possibly related to the outburst of an ice-, moraine- or rockfall-dammed lake could be the reason for the exceptional megaturbidite. Such a process has been proposed for two exceptional graded layers in Lake Constance, which have been linked to the outburst of two lakes produced by the Flims and Tamins Rockfalls, respectively (Schneider et. al. 2004).

8. Trigger Mechanism

One of the most remarkable characteristics of the mass-flow deposits in the subsurface of Lake Lucerne is the occurrence of several horizons with multiple coeval mass-flow and megaturbidite deposits (Figs 7, 10). Seventy-five of the total 91 mapped mass-flow deposits relate to 6 multiple mass-movement horizons showing that regional trigger mechanisms are important. Multiple mass movement deposits have been shown to be a common geological signature of strong historic earthquakes, both in subaerial (Keefer 2002; Becker & Davenport 2003; Harp et al. 2003) and subaqueous environments (Locat et al. 2003; Skinner & Bornhold 2003). In Lake Lucerne, the youngest multiple mass-movement horizon (Event C) relates to the 1601 A.D. $M_w \sim 6.2$ earthquake and comprises 13 coeval mass-flow deposits, which are overlain by two megaturbidites in the center of the Chrüztrichter and Vitznau basins. Distinct, more than 6 m-high failure scars on the subaqueous slopes
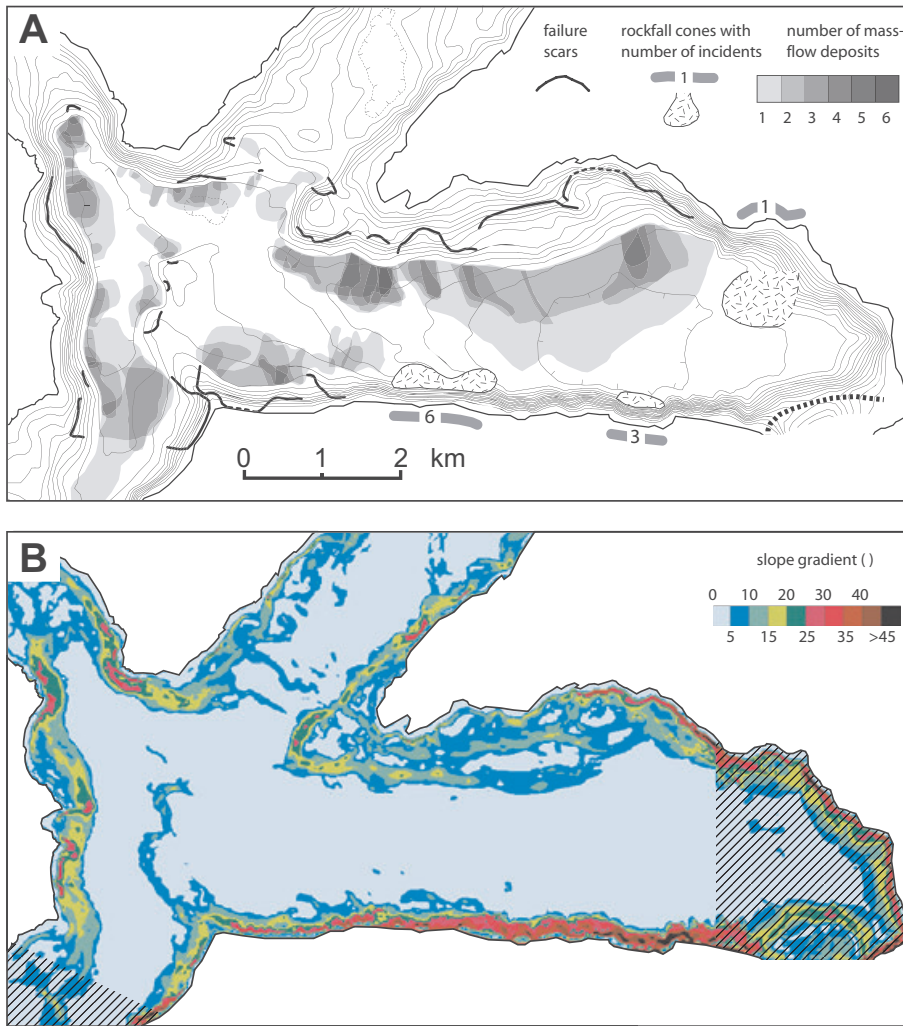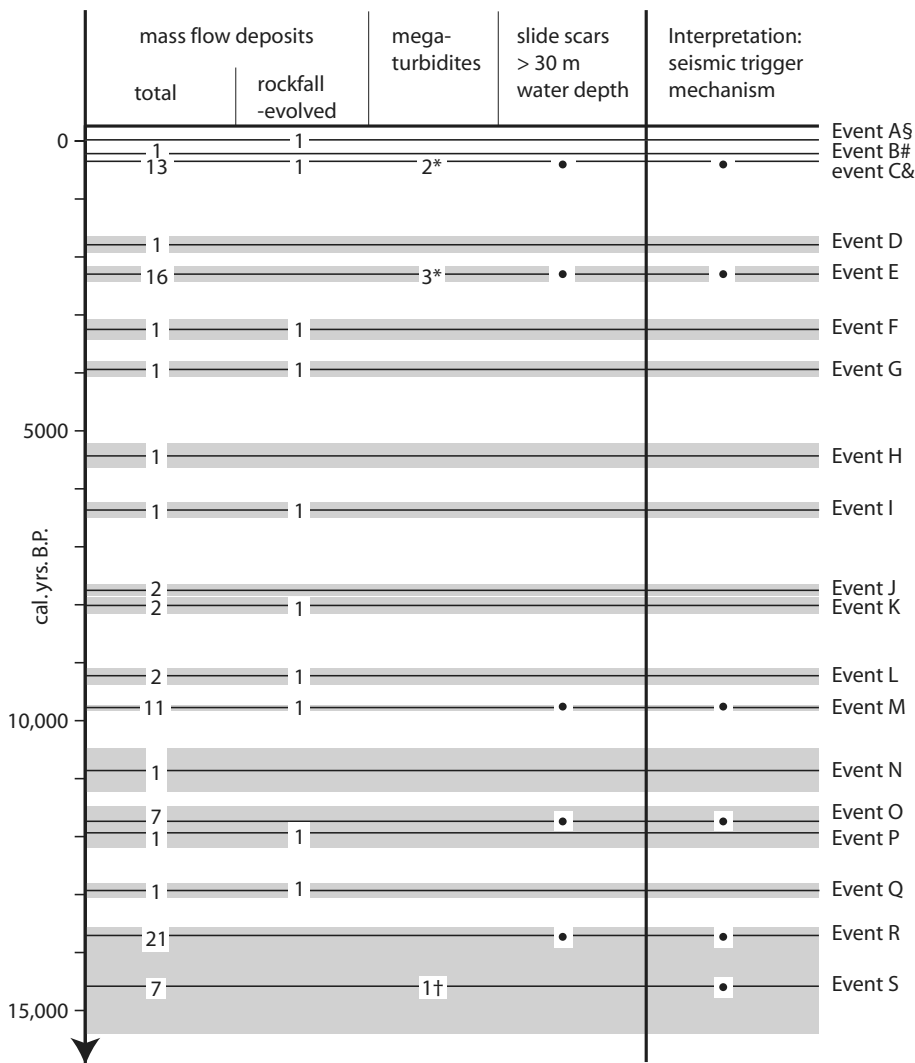
Fig. 9. A. Spatial distribution of identified slide scars, rockfall cones and mass-flow deposits. Gray shadings indicate the total number of identified mass-flow deposits at the foot of slopes with sub-aqueous failure scars. The number of rockfall-evolved mass-flow deposits related to each of the three rockfall cones is indicated next to the cones. B. Slope gradients of the studied basins as calculated from the seismic data. In the hatched area, the spacing of the seismic lines is insufficient for an accurate determination of the slope gradient. Some artefacts also occur in the immediate proximity of the shoreline.

point towards subaqueous sliding as the dominant primary mass-movement process. One of the 1601 A.D. mass-flow deposits directly lies at the foot of a rockfall cone and is, therefore, interpreted as rockfall-evolved. Historical data, indeed, describe a rockfall on Bürgenstock Mountain, which caused a wave in the Vitznau Basin (Cysat 1969; Schwarz-Zanetti et al. 2003). The location of the identified rockfall deposit fits well to a locality named "an der Risi" (in English: at the place of the rockfall) on a detailed map of Lake Lucerne from 1645 A.D. (Cysat 1645).

Historic Event C shows the typical signature of a strong earthquake in Lake Lucerne and points towards a high suscep-tibility of the subaqueous slopes to multiple earthquake-in-duced sliding (Figs 7; 10). Prehistoric multiple mass-movement horizons in Lake Lucerne are, therefore, likely to be the prod-uct of strong seismic shocks as well and can be used to recon-struct the prehistoric earthquake history. Prehistoric Events E, M, O, R and S each comprise seven or more coeval mass-flow deposits and are, thus, interpreted as the result of strong earth-

quake shaking (Figs 7, 10). In contrast, mass-flow deposits lacking more than one coeval counterpart are regarded as trig-gered either by an aseismic process or by a minor seismic shock. Strong earthquakes can be excluded as trigger mecha-nism as they would destabilize multiple slopes at the same time.

For testing the earthquake triggering hypothesis, we further analyzed the multiple mass-movement horizons and tried to systematically exclude possible non-earthquake triggers, i.e. overloading and oversteepening of subaqueous slopes, regional flood events, loading by wind-induced surface waves and lake level variations. Overloading or oversteepening of different slopes of various orientation and water depths are unlikely to occur synchronously, particularly in the studied basins, which are characterized by low fluvial input. Flood events may trigger subaerial landslides, subaerial debris flows and hyperpycnal flows within a short time period all around the lake. Although such subaerial events may reach the lake and are capable of eroding submerged slopes along their pathway, they cannot ex-

mass flow deposits		mega-turbidites	slide scars > 30 m water depth	Interpretation: seismic trigger mechanism	
total	rockfall-evolved				
1	1				Event A§
1					Event B#
13	1	2*	•	•	event C&
1					Event D
16		3*	•	•	Event E
1	1				Event F
1	1				Event G
1					Event H
1	1				Event I
2					Event J
2	1				Event K
2	1				Event L
11	1		•	•	Event M
1					Event N
7			•	•	Event O
1	1				Event P
1	1				Event Q
21			•	•	Event R
7		1†		•	Event S

cal. yrs. B.P. (vertical axis: 0, 5000, 10,000, 15,000)

*Megaturbidite related to subaqueous sliding and to related tsunami/seiche waves
†Megaturbidite related to major delta collapse or outburst of naturally-dammed lake
§Hist. rockfall, 1964 A.D. (Huber, 1980; Lemcke, 1992)
#Continuation of hist. subaerial landslide, 1795 A.D. (Pfyffer, 1795; Zwyer, 2006)
&Hist. earthquake, 1601 A.D., M_w ~ 6.2 (Siegenthaler et. al., 1987; Schwarz-Zanetti et. al., 2003)

Fig. 10. Stratigraphical distribution of identified event horizons in Chrüztrichter and Vitznau Basins. Shadings indicate the error bars. Number and type of deposits, as well as the inferred trigger mechanism, are shown for each event horizon.

plain deeply submerged scars and/or deposits at the foot of subaqueous hills in longer distance from the shoreline. Such features have been observed for all multiple mass-movement horizons with the exception of event S (Figs 6, 10). Extreme wind events may rework and destabilize the shallow zones of the lake. The maximum water depth, which may be influenced by wind-induced surface waves, can be calculated for certain fetches (horizontal distance over which a wave-generating wind blows) and wind velocities (Hakanson & Jansson 1983). A worst case scenario for the study area with stable wind velocities of 40 m/s and an effective fetch of 5 km revealed wave amplitudes of 1 m, wavelengths of 37 m and a wave base (l/2 wavelength) of 18.5 m. Sediment in water depths >30 m below the present lake level is, therefore, unlikely to be affected by wind

activity, even at times when the lake level was 9 m lower than today (Kopp 1938; Eberschweiler 2003). It also seems unlikely that the probably stepwise rise of lake level since mid Holocene times triggered numerous coeval slides in the deep water.

The tsunami waves associated with major rockfall or subaqueous slide events may erode parts of the shore and will induce rapid lake level changes, which will potentially initiate secondary mass flows. Events K, L and M include major rockfalls and mass-flow deposits at the foot of the slopes opposite the rockfall cliff. Out of these three horizons, a seismic trigger mechanism is only assigned to Event M, which comprises mass-flow deposits at other locations than just opposite the rockfall cliff and includes a slide scar in more than 70 m water depth.

It remains unclear, whether the megaturbidite associated to event S results from a delta collapse or from the outbreak of a naturally dammed lake. Both, delta collapses and the outbreak of dammed lakes can be, but don't have to be related to earthquakes. Our assignment of a seismic trigger to event S is based on the fact that the megaturbidite correlates to 7 mass-flows in different parts of the lake.

The temporal distribution of the 6 horizons, which are interpreted as remnants of strong earthquakes, is highly irregular with four out of six events occurring between 9800 and 15,000 cal. yr B.P. (Fig. 10). The higher frequency before 9800 cal. yr B.P. could potentially be related to isostatic rebound after retreat of the alpine glaciers (Stewart et al. 2000, and references therein).

The number and size of mass-flow deposits associated to an event horizon do not necessarily reflect the intensity of seismic shaking. Particularly if two earthquake shocks of similar size appear within a short period, the number and size of the mass-flow deposits related to the second shock will, most probably, be smaller. To test the results from this study and to estimate magnitudes and epicenters, it is crucial to investigate a series of archives within a region and to map out the regional distribution of earthquake traces related to specific prehistoric events. The identification of mass-flow deposits and soft-sediment deformation structures related to the 1601 A.D. earthquake in Lake Lungern, Lake Seelisberg and Lake Baldegg shows that the smaller lakes in the vicinity of Lake Lucerne are capable of recording earthquake activity (Monecke et al. 2004). Paleoseismic investigations of prehistoric sediments in these lakes are given by Monecke et al. (2006, this volume). In a recent study three multiple mass-movement horizons have been identified in Lake Zurich (Strasser et al. 2006). The age ranges of these events overlap with Events E, O and R in Lake Lucerne strengthening the hypothesis of earthquake triggering and allowing for estimates of magnitudes and epicenters.

9. Conclusion

(1) Combined high-resolution seismic and core studies of the subsurface of lakes enable identification and dating of stacked mass-movement deposits and allow for the determination of their type, distribution and frequency. In this way, the historic mass-movement event catalogue can be extended to prehistoric times and low frequency events can be included in the natural hazard assessment of a region.

(2) Subaqueous slides leave failure scars on the slopes and wedge-shaped mass-flow deposits with a chaotic-to-transparent seismic facies in the subjacent basin plain. Size and frequency of subaqueous slides largely depend on slope gradients. In the studied basins of Lake Lucerne, the most frequent and extensive deposits appear beneath slopes with moderate inclinations of 10–20°. Slopes with inclinations smaller than 10° barely failed in the past and slopes steeper than 25° seem to be too steep to accumulate enough sediment for major sliding.

(3) Rockfalls build up basin-marginal cones with hum-

mocky surfaces that are not penetrated by the seismic signal, but typically produce diffractions and some high-amplitude reflections. Stacked mass-flow deposits at the foot of a rockfall cone point towards repeated rockfalls from the same cliff. Our data reveal a major rockfall event at the Rigi Mountain and repeated rockfall activity along two zones of the Bürgenstock Mountain. Two historical examples indicate that the main hazard caused by rockfalls from the Bürgenstock cliff arises from waves induced by rockfall-impact on the lake. Most of the prehistoric deposits are larger compared to their historic counterparts and are, therefore, likely to have initiated equal or larger impact waves.

(4) Six multiple mass-movement horizons have been identified, each comprising 7 or more coeval deposits. The youngest of these events relates to the 1601 A.D. $M_w \sim 6.2$ earthquake. By analogy, the five older multiple mass-movement horizons are interpreted as remnants of strong prehistoric earthquakes. Four of the five prehistoric horizons include slide scars in water depths >30 m, providing further evidence for a seismic trigger mechanism, as even extreme winds or rainfall events including widespread subaerial debris-flow activity will not produce failure scars on non-delta slopes in such water depths. The temporal distribution of the multiple mass-movement horizons indicates an irregular occurrence of strong earthquakes in the past 15,000 years, with enhanced activity during Late Glacial and early Holocene times.

Acknowledgements

REFERENCES

BECKER, A. & DAVENPORT, C.A. 2003: Rockfalls triggered by the AD 1356 Basle Earthquake. Terra Nova 15, 258–264.

BILLETER, J. 1916: Aus der Chronik des Pfarrers Jakob Billeter von Aegeri. In: XXII. Neujahrsblatt Uri, Verein für Geschichte und Altertümer von Uri, Altdorf, 43.

BLIRKA, L.H., LONGVA, O., BRAATHEN, A. & ANDA, E., DEHLS, J. & STALSBERG, K. in press: Rock-slope failures in Norwegian fjord areas: examples, spatial distribution and temporal pattern. In: Landslides from Massive Rock Slope Failure (Ed. by EVANS, S.G., SCARAWCIA MUGNOZZA, G., STROM, A.L. & HERMANNS, R.L.), Springer, Dordrecht.

BOUMA, A.H. 1987: Megaturbidite: An Acceptable Term? Geo-Marine Letters 7, 63–67.

BUSSMANN, F. 2006: The sediments of Lake Lauerz – a new approach to establish the timing of the Rossberg landslide succession and the chronology of exceptional rainfall events. Unpublished Diploma Thesis ETH Zurich, 82 pp.

BUXTORF, A., 1916: Geologische Vierwaldstättersee-Karte 1:50 000, Schweizerische Geologische Kommission, Bern.

BÜNTI, J.L. 1914: Aus der Chronik des Landammann Joh. Lorenz Bünti von Stans. In: XX. Neujahrsblatt Uri, Verein für Geschichte und Altertümer von Uri, Altdorf, 8–9.

CHAPRON, E., BECK, C., POURCHET, M. & DECONINCK, J.F. 1999: 1822 earthquake-triggered homogenite in Lake Le Bourget (NW Alps). Terra Nova 11, 86–92.

CYSAT, J.L. 1645: Wahre Abbildung der 4 Waldstätten See. Historische Karte. Clemens Beutler fecit., Luzern, 1645.

CYSAT, R. 1969: Collectanea Chronica und denkwürdige Sachen pro Chronica Lucernensi et Helvetiae. Erster Band, Zweiter Teil. In: Quellen und Forschungen zur Kulturgeschichte von Luzern und der Innerschweiz (Ed. by SCHMID, J.). Diebold Schilling Verlag, Luzern, 882–888.

EBERSCHWEILER, B. 2003: Jungsteinzeitliche Ufersiedlung in Stansstad-Kehrsiten NW. Gutachten des Amtes für Städtebau der Stadt Zürich. Abteilung Unterwasserarchäologie + Labor für Dendrochronologie, Zürich, 12 pp.

FÄH, D., GIARDINI, D., BAY, F., BERNARDI, F., BRAUNMILLER, J., DEICHMENN, N., FURRER, M., GANTNER, L., GISLER, M., ISENEGGER, D., JIMENEZ, M.J., KAESTLI, P., KOGLIN, R., MASCIADRI, V., RUTZ, M., SCHEIDEGGER, C., SCHIBLER, R., SCHORLEMMER, D., SCHWARTZ-ZANETTI, G., STEIMEN, S., SELLAMI, S., WIEMER, S. & WOESSNER, J. 2003: Earthquake Catalogue Of Switzerland (ECOS) And The Related Macroseismic Database. Eclogae Geologicae Helvetiae 96, 219–236.

FINCKH, P., KELTS, K. & LAMBERT, A. 1984: Seismic stratigraphy and bedrock forms in perialpine lakes. Geological Society of America Bulletin 95, 1118–1128.

FRITZ, H.M. 2002: Initial phase of landslide generated impulse waves. Dissertation ETH Zürich, 249 pp.

GILLI, A., ANSELMETTI, F.S., ARIZTEGUI, D. & MCKENZIE, J.A. 2003: A 600-year sedimentary record of flood events from two sub-alpine lakes (Schwendiseen, Northeastern Switzerland). Eclogae Geologicae Helvetiae 96, 49–58.

HAJDAS, I., IVY, S.D., BEER, J., BONANI, G., IMBODEN, D., LOTTER, A.F., STURM, M. & SUTER, M. 1993: AMS radiocarbon dating and varve chronology of Lake Soppensee: 6000 to 12000 ^{14}C years BP. Climate Dynamics 9, 107–116.

HAJDAS, I., IVY, S.D., BONANI, G., LOTTER, A.F. ZOLITSCHKA, B. & SCHLUECHTER, C. 1995: Radiocarbon Age of the Laacher See Tephra: 11,230 ± 40 BP. Radiocarbon 37, 149–154.

HAKANSON, L. & JANSSON, M. 1983: Principles of Lake Sedimentology. The Blackburn Press, Caldwell, 316 pp.

HARP, E.L., JIBSON, R.W., KAYEN, R.E., KEEFER, D.K., SHERROD, B.L., CARVER, G.A., COLLINS, B.D., MOSS, R.E.S. & SITAR, N. 2003: Landslides and liquefaction triggered by the M 7.9 Denali Fault earthquake of 3 November 2002. GSA Today 13, 4–10.

HEIM, A. 1876: Bericht und Expertengutachten über die im Februar und September 1875 in Horgen vorgekommenen Rutschungen. Bericht der Expertenkommission. Hofer und Burgen, Zürich, 22 pp.

HEIM, A. 1888: Die Katastrophe von Zug 5. Juli 1887. Gutachten der Experten. Hofer und Burgen, Zürich, 57 pp.

HEIM, A. 1932: Bergsturz und Menschenleben. Beiblatt zur Vierteljahresschrift der Naturforschenden Gesellschaft in Zürich, Beer & Co., Zürich, 218 pp.

HSÜ, K.J. & KELTS, K. 1985: Swiss Lakes as a Geological Laboratory. Naturwissenschaften 72, 315–321.

HUBER, A. 1980: Schallwellen in Seen als Folge von Felsstürzen. Mitteilungen der Versuchsanstalt für Wasserbau, Hydrologie und Glaziologie, Zürich, 222 pp.

KAUFMANN, F.J. 1872: Rigi und Molassegebiet der Mittelschweiz, geologisch aufgenommen und beschrieben, In Commission bei J. Dalp, Bern, 534 pp.

KANTON LUZERN 2006a: Überarbeitete Gefahrenkarte Weggis nach dem Unwetter von August 2005. Karte der Phänomene Bereich Dorf. LAWA (Dienststelle Landwirtschaft und Wald), Luzern.

KANTON LUZERN 2006b: Überarbeitete Gefahrenkarte Weggis nach dem Unwetter von August 2005. Karte der Phänomene Bereich Rigi Kaltbad – Lützelau. LAWA (Dienststelle Landwirtschaft und Wald), Luzern.

KEEFER, D.K. 2002: Investigating landslides caused by earthquakes – A historical review. Surveys in Geophysics 23, 473–510.

KELTS, K., BRIEGEL, U., GHILARDI, K. & HSÜ, K.J. 1986: The limnogeology-ETH coring system. Schweizerische Zeitschrift für Hydrologie 48, 104–115.

KELTS, K. & HSÜ, K.J. 1980: Resedimented facies of 1875 Horgen slumps in Lake Zurich and a process model of longitudinal transport of turbidity currents. Eclogae Geologicae Helvetiae 74, 271–281.

KOPP, J. 1936: Die Bergstürze des Rossberges. Eclogae Geologicae Helvetiae 29, 490–493.

KOPP, J. 1938: Der Einfluss des Krienbaches auf die Gestaltung des Luzernersees und die Hebung des Seespiegels des Vierwaldstättersees. Eclogae Geologicae Helvetiae 31, 376–378.

LEMCKE, G. 1992: Ablagerungen aus Extremereignissen als Zeitmarken der Sedimentationsgeschichte im Becken von Vitznau/Weggis (Vierwaldstättersee, Schweiz). Unpublizierte Diplomarbeit Georg-August-Universität Göttingen, 154 pp.

LOCAT, J., MARTIN, F., LEVESQUE, A.J., LOCAT, P., LEROUEIL, S., KONRAD, J.M., URGELES, R., CANALS, M. & DUCHESNE, M.J. 2003: Submarine mass movements in the Upper Saguenay Fjord (Québec – Canada), triggered by the 1663 earthquake. In: Submarine Mass Movements and Their Consequences: 1st International Symposium (Ed. by LOCAT, J., MIENERT, J. & BOISVERT, L.). Kluwer, Dordrecht, 509–519.

LONGVA, O., JANBU, N., BLIKRA, L.H. & BØE, R. 2003. The 1996 Finneidfjord Slide; Seafloor Failure and Slide Dynamics. In: Submarine Mass Movements and Their Consequences: 1st International Symposium (Ed. by LOCAT, J., MIENERT, J. & BOISVERT, L.). Kluwer, Dordrecht, 531–538.

MAYER, B. & SCHWARK, L. 1999: A 15000-year stable. isotope record from sediments of Lake Steisslingen. Southwest Germany. Chemical Geology 161, 315–337.

MERKT, J. 1971: Zuverlässige Auszählung von Jahresschichtung in Seesedimenten mit Hilfe von Gross-Dünnschliffen. Archiv für Hydrobiologie 69, 145–154.

MONECKE, K., ANSELMETTI, F.S., BECKER, A., STURM, M. & GIARDINI, D. 2004: The record of historic earthquakes in lake sediments of Central Switzerland. Tectonophysics 394, 21–40.

MONECKE, K., ANSELMETTI, F.S., BECKER, A., SCHNELLMANN, M., STURM, M. & GIARDINI, D., 2006: Earthquake-induced deformation structures in lake deposits – A Late Pleistocene to Holocene paleoseismic record for Central Switzerland. Eclogae Geologicae Helvetiae 99, 343–362.

MULDER, T. AND COCHONAT, P. 1996: Classification of offshore mass movements. Journal of Sedimentary Research 66, 43–57.

NARDIN, T.R., HEIN, F.J., GORSLINE, D.S. AND EDWARDS, B.D. 1979: A review of mass movement processes, sediment and acoustic characteristics, and contrasts in slope and base-of-slope systems versus canyon-fan-basin floor systems. In: Geology of continental slopes (Ed. by L.J. DOYLE and O.H. PILKEY), International Association of Sedimentologists Special Publications 27, 61–73.

PFYFFER, J., 1795: Plan der Rutschung von Weggis vom 15./16. Juli 1995. Im Besitz der Gemeinde Weggis.

PRIOR, D.B., BORNHOLD, B.D. & JOHNS, M.W. 1984: Depositional characteristics of a submarine debris flow. Journal of Geology 92, 707–727.

SCHNEIDER, J.-L., POLLE, N., CHAPRON, E., WESSELS, M. AND WASSMER, P., 2004: Signature of Rhine Valley sturzstrom dam failures in Holocene sediments of Lake Constance, Germany. Sedimentary Geology 169, 75–91.

SCHNELLMANN, M., ANSELMETTI, F.S., GIARDINI, D. & MCKENZIE, J.A. & WARD, S.N. 2002: Prehistoric earthquake history revealed by lacustrine slump deposits. Geology 30, 1131–1134.

SCHNELLMANN, M., ANSELMETTI, F.S., GIARDINI, D. & MCKENZIE, J.A. 2005: Mass movement-induced fold-and-thrust belt structures in unconsolidated sediments in Lake Lucerne (Switzerland). Sedimentology 52, 271–289.

SCHWARTZ-ZANETTI, G., DEICHMANN, N., FÄH, D., GIARDINI, D., JIMENEZ, M.J., MASCIADRI, V., SCHIBLER, R. & SCHNELLMANN, M. 2003: The Earthquake in Unterwalden on September 18, 1601 – A Historico-Critical Macroseismic Evaluation. Eclogae Geologicae Helvetiae 96, 441–450.

SHILTS, W.W., & CLAGUE, J.J. 1992: Documentation of earthquake-induced disturbance of lake sediments using subbottom acoustic profiling. Canadian Journal of Earth Sciences 29, 1018–1042.

SHOTYK, W., WEISS, D., APPLEBY, G.B., CHEBURKIN, A.K., FREI, R., GLOOR, M., KRAMERS, J.D., REESE, S. & VAN DER KNAAP, W.O. 1998: History of Atmospheric Lead Deposition Since 12,370 14C yr BP from a Peat Bog, Jura Mountains, Switzerland. Science 281, 1635–1640.

SIEGENTHALER, C., FINGER, W., KELTS, K. & WANG, S. 1987: Earthquake and seiche deposits in Lake Lucerne, Switzerland. Eclogae Geologicae Helvetiae 80, 241–260.

SIEGENTHALER, C., & STURM, M. 1991a: Die Häufigkeit von Ablagerungen extremer Reuss-Hochwasser. Die Sedimentationsgeschichte im Urnersee seit dem Mittelalter. In: Ursachenanalyse der Hochwasser 1987. Ergebnisse der Untersuchungen. Mitteilungen des Bundesamtes für Wasserwirtschaft 4, 127–139.

SIEGENTHALER, C., & STURM, M. 1991b: Slump induced surges and sediment transport in Lake Uri, Switzerland. Verh. Int. Ver. Limnol. 24, 955–958.

SKINNER, M.R. & BORNHOLD, B.D. 2003: Slope Failures and Paleoseismicity, Effingham Inlet, Southern Vancouver Island, British Columbia, Canada. In: Submarine Mass Movements and Their Consequences: 1st International Symposium (Ed. by LOCAT, J., MIENERT, J. & BOISVERT, L.). Kluwer, Dordrecht, 375–382.

SLETTEN, K., BLIKRA, L.H., BALLANTYNE, C.K., NESJE, A. & DAHL, S.O. 2003: Holocene debris flows recognized in a lacustrine sedimentary succession: sedimentology, chronostratigraphy and cause of triggering. Holocene 13, 907–920.

STEWART, I.S., SAUBER, J. & ROSE, J. 2000: Glacio-seismotectonics: Ice sheets, crustal deformation and seismicity. Quaternary Science Reviews 19, 1367–1389.

STRASSER, M., ANSELMETTI, F.S., FÄH, D., GIARDINI, D. & SCHNELLMANN, M. 2006: Magnitudes and source areas of large prehistoric northern Alpine earthquakes revealed by slope failures in lakes. Geology 34, 1005–1008.

STUIVER, M. & REIMER, P.J. 1993: Extended ^{14}C database and revised CALIB radiocarbon calibration program. Radiocarbon 35, 215–230.

STURM, M. & LOTTER, A.F. 1995: Lake sediments as environmental archives. EAWAG News 38E, 6–9

VISCHER, D.L. 1986: Rockfall-induced waves in reservoirs. Water Power & Dam Construction 39, 45–48.

ZIMMERMANN, J. 1913: Vitznau am Fusse der Rigi. Sammlung von Schweizer Monographien 2, 8–19.

ZWYER, T. 2006: Die unterseeische Fortsetzung der Schlammlawine von Weggis im Jahre 1795. Unpublished Bachelor Thesis. ETH Zürich. 74 pp.